Bioorg. Med. Chem. 30 (2021) 115964

Contents lists available at ScienceDirect

Bioorganic & Medicinal Chemistry

journal homepage: www.elsevier.com/locate/bmc

Lead optimization of 2-hydroxymethyl imidazoles as non-hydroxamate LpxC inhibitors: Discovery of TP0586532

Fumihito Ushiyama *, Hajime Takashima, Yohei Matsuda, Yuya Ogata, Naoki Sasamoto, Risa Kurimoto-Tsuruta, Kaori Ueki, Nozomi Tanaka-Yamamoto, Mayumi Endo, Masashi Mima, Kiyoko Fujita, Iichiro Takata, Satoshi Tsuji, Haruhiro Yamashita, Hirotoshi Okumura, Katsumasa Otake, Hiroyuki Sugiyama

Taisho Pharmaceutical Co., Ltd, 1-403 Yoshino-Cho, Kita-Ku, Saitama 331-9530, Japan

ARTICLE INFO

Keywords:
LpxC
Non-hydroxamate
Antibacterial agent
Gram-negative bacteria
carbapenem-resistant Enterobacteriaceae
Lead optimization

ABSTRACT

Infectious diseases caused by resistant Gram-negative bacteria have become a serious problem, and the development of therapeutic drugs with a novel mechanism of action and that do not exhibit cross-resistance with existing drugs has been earnestly desired. UDP-3-*O*-acyl-*N*-acetylglucosamine deacetylase (LpxC) is a drug target that has been studied for a long time. However, no LpxC inhibitors are available on the market at present. In this study, we sought to create a new antibacterial agent without a hydroxamate moiety, which is a common component of the major LpxC inhibitors that have been reported to date and that may cause toxicity. As a result, a development candidate, **TP0586532**, was created that is effective against carbapenem-resistant *Klebsiella pneumoniae* and does not pose a cardiovascular risk.

1. Introduction

In recent years, drug-resistant Gram-negative bacteria have been recognized as a global threat.[1,2] The World Health Organization (WHO) published the Global Action Plan on Antimicrobial Resistance in 2015; in 2017, they published a list of drug-resistant bacteria that require the immediate development of new antimicrobial agents.[3,4] Until now, β-lactam, quinolone, and aminoglycoside drugs, etc., have been used as effective drugs for the treatment of Gram-negative bacterial infections. However, a large number of Enterobacteriaceae such as *Klebsiella pneumoniae* and *Escherichia coli* resistant to these drugs have been reported in clinical practice.[5,6] Among them, carbapenem-resistant Enterobacteriaceae (CRE) exhibit strong resistance to many drugs including carbapenem antibiotics, which are regarded as important agents in the treatment of infectious diseases.[7] CRE infection has a high mortality rate, and its incidence is increasing globally.[8] CRE infections are presently treated with combinations of antimicrobial agents to which the strain is susceptible, but treatment has been difficult in some cases.[9] Therefore, the development of therapeutic agents with novel mechanisms of action is desired.[10]

UDP-3-*O*-acyl-*N*-acetylglucosamine deacetylase (LpxC) is a zinc-dependent deacetylase that catalyzes the essential step in the biosynthesis of lipid A, which is a component of lipopolysaccharide (LPS) in Gram-negative bacteria.[11] LpxC is a well-validated pharmacological target, and much effort has been devoted to the creation of LpxC inhibitors over the past 20 years.[12] However, there are still no inhibitors of LpxC on the market.[13] Previous LpxC inhibitors contained hydroxamic acid at the zinc coordination site.[13] However, this structure often increases the risk of toxicity.[14,15] ACHN-975 (Achaogen)[16] and RC-01 (FUJIFILM Toyama Chemical),[17] which were leading LpxC inhibitors that both contained a hydroxamic acid moiety, reached the clinical trial stage, but the development of both compounds was terminated in Phase 1.[18,19] (see Fig. 1).

Therefore, we sought to create LpxC inhibitors that do not contain a hydroxamic acid—and consequently an increased risk of toxicity.[14,15] The creation of a novel chemical class of LpxC inhibitors different from conventional LpxC inhibitors would enable new treatment options. Our fragment-based drug discovery (FBDD) method showed that 2-(1*S*-hydroxyethyl)-imidazole derivatives could be an alternative to compounds containing a hydroxamic acid moiety.[20] Among them, compound **1** had an attractive antibacterial activity against *E. coli* of 0.5 μg/mL.[20] However, compound **1** also had a high protein binding ability

* Corresponding author.
E-mail address: f-ushiyama@taisho.co.jp (F. Ushiyama).

https://doi.org/10.1016/j.bmc.2020.115964
Received 17 November 2020; Received in revised form 14 December 2020; Accepted 16 December 2020
Available online 29 December 2020

(Table 1) and was not expected to exhibit *in vivo* efficacy. Therefore, we sought an approach that would reduce the human protein binding of compound **1** while maintaining its antibacterial activity against Enterobacteriaceae. In practice, we explored and optimized the SAR of the tail site located in the solvent-exposed region, the introduction of a polar group adjacent to the imidazole moiety, and the hydrophobic tunnel site. Compounds with reduced protein binding were evaluated *in vivo* using efficacy tests and safety pharmacology tests involving the guinea pig cardiovascular system under anesthesia. Based on the results of the above examinations, **TP0586532**, which contains a carboxy group at the termination of the tail site, was selected and profiled.

2. Results and discussion

2.1. Design strategy

In the present study, compound **1**, which was discovered in a previously reported study,[20] was used as the lead compound in an effort to create novel non-hydroxamate LpxC inhibitors. The most important characteristic of lead compound **1** is that the zinc coordination site is constructed using 2-(1*S*-hydroxyethyl)-imidazole. Specifically, compound **1** coordinates with zinc at a secondary hydroxy group and the nitrogen atom of imidazole. On the other hand, most LpxC inhibitors reported to date, such as CHIR-090[21] (Fig. 2), contain a hydroxamate moiety at this site, and concerns regarding mutagenicity[14,15] exist because of their distinctive structures.

Similar to previously reported LpxC inhibitors, compound **1** fills the target hydrophobic tunnel site of LpxC with a linear lipophilic acetylene and a benzene ring. Also, a space exists in the solvent-exposed area of the molecule where a tail with adjustable physicochemical properties could be introduced.

Lead compound **1** exerted antibacterial activities against *E. coli* ATCC 25922 and *K. pneumoniae* ATCC 13883 at concentrations of 0.5 μg/mL and 2 μg/mL, respectively, but the serum protein binding ability for both human and mouse proteins was >99.5% (Table 1). Thus, we attempted to create a novel non-hydroxamate LpxC inhibitor with *in vivo* efficacy by reducing the protein binding while maintaining or improving the antibacterial activity.

2.2. First optimization based on compound 1

Based on information for lead compound **1**, the tail and the hydrophobic tunnel site (part A) were examined (Table 1).

We started replacing the tail part of **1** with hydrophilic part to reduce protein binding. Compound **2**, which contained hydroxypropylazetidine indicated considerable reduction of the protein binding; however both the enzyme inhibitory and antibacterial activities against *E. coli* and *K. pneumoniae* were also attenuated, as was the case with other reported LpxC inhibitors.[22] Piperazine **3** had a stronger antibacterial activity against *K. pneumoniae* than lead compound **1**; a reduction in protein binding was also confirmed. Even though, in a murine systemic infection model caused by infection with *K. pneumoniae* 4102, mice treated with 25 mg/kg of compound **3** only had a 17% survival rate at 7 days after inoculation. By contrast, compound **4**, in which the positions of the benzene ring and the acetylene moiety of lead compound **1** were exchanged, had almost the same antibacterial activity as lead compound **1**, while a clear reduction in protein binding was observed. To verify the effect of the ethynyl-benzene replacement, cocrystals of compound **5** (a racemate of lead compound **1**)[20] and compound **4** were compared (Fig. 3). This examination confirmed that the amino acid residue of Ile197 was considerably more induced-fit in compound **4** than in compound **5** and that this residue was closer to the hydrophobic tunnel region. A similar phenomenon has been reported for LpxC inhibitors [23,24]; this induced-fit increases the spatial tolerance of the hydrophobic tunnel exit on the tail side, making it easier to deploy a wide range of tail types.

2.3. Second optimization based on compound 4

Further prioritization was made in consideration of the results shown in Fig. 3 and the reduction in protein binding enabled by the conversion of lead compound **1** to compound **4**. Namely, we decided to investigate the derivatives of compound **4**, in which the hydrophobic tunnel is composed of the sequence, beginning from the tail side, "tail-acetylene-phenyl". The results of the optimization of the tail and part B (corresponding to the isoxazole site) are shown in Table 2.

Further examination of the tail site revealed that the introduction of the rigid parts tended to favor antibacterial activity over flexible alkyl chains such as compound **4**. In fact, cyclopropylamine **6** showed an equivalent or better antibacterial activity against *E. coli* and *K. pneumoniae* than compound **4**. The serum protein binding to human and mouse proteins was also reduced to 93.0% and 90.1%, respectively. Furthermore, in a murine systemic infection model, the survival rate at 7 days was 67%, indicating an *in vivo* efficacy. Also, compounds **7** and **8**, in which bicyclopentylamine and cyclobutyl alcohol were respectively introduced into the tail, had stronger antibacterial activities against *E. coli* and *K. pneumoniae* than compound **6**. However, a reduction in serum protein binding was not observed, and no *in vivo* efficacy was confirmed. Compound **9**, which contained azabicyclohexane at the tail site, had almost the same antibacterial activity and protein binding ability as compound **6** but was inferior in terms of *in vivo* efficacy when evaluated using a murine systemic infection model.

In addition, derivatives in which the nitrogen and oxygen atoms of isoxazole were exchanged were also synthesized and evaluated. When compounds **6** and **10** (NO-replacement form) were compared, compound **10** showed reduced protein binding, but both its enzyme inhibitory activity and its antibacterial activity were weakened. The other NO-replacement compounds (**11** and **12**) were found to have protein binding abilities that were lower than or equal to those of compounds **7** and **9**, which had the same respective tail types. Compounds **11** and **12** also had improved antibacterial activities and higher protein binding when compared with compound **10**. Although compound **12** had the strongest antibacterial activity amongst the NO-replacements, its *in vivo* efficacy was inferior to that of compound **6** when examined using a murine systemic infection model.

As described above, compound **6**, which was one of the most promising compounds, had the strongest *in vivo* efficacy in the murine

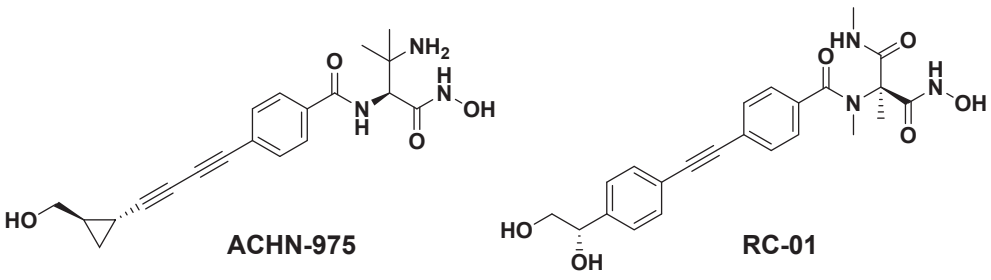

Fig. 1. LpxC inhibitors that advanced to the clinical stage of development.

systemic infection model (Table 2). However, the maximum tolerated dose in mice, as determined using a single intravenous administration study of compound **6** in mice, was 50 mg/kg, resulting in a narrow margin of efficacy. Also, convulsive symptoms in mice were confirmed, and there were concerns about the effects of compound **6** on the central nervous system. Therefore, studies were conducted to further improve drug efficacy, reduce central transferability, and minimize off-target effects. Cocrystal information for compound **4** suggested that a substituent could be introduced into the imidazole-adjacent position. As shown in Fig. 2, a space where a side chain could be extended is present in lead compound **1**. In contrast, it would be difficult to extend a side chain while maintaining the existing binding mode on the back side of the paper. Such side chains would likely form new interactions with amino acid residues or via water. In addition, the introduction of polar groups was expected to reduce protein binding. Thus, we next introduced various side chains to the adjacent position of imidazole, selected the most promising aminomethyl group, and performed combination synthesis with the attractive tails that had been obtained so far. Furthermore, we actively introduced neutral and acidic components into the tail site and searched for promising compounds (Table 3).

Compound **13** had a weaker antibacterial activity than compound **6**, which had the same tail, because of a structural conversion introduced by an aminomethyl group. Compounds **14** and **15** had comparable or slightly attenuated antibacterial activities compared with compounds **7** and **8** listed in Table 2, but their human protein binding abilities were improved by 5% or more. Furthermore, compound **17** had a human protein binding of less than 80% even though it had no basic nitrogen atom at its tail site. Among other aminomethyl derivatives, a number of compounds, such as compound **18**, with a human protein binding of less than 80% were obtained. In the hopes of reducing protein binding and avoiding the toxicity seen in compound **6**, a carboxy group, which is an acidic functional group, was introduced at the tail site in compound **19** (**TP0586532**), which did not have an aminomethyl group. Compound **19** (**TP0586532**) had the same antibacterial activity as that of the compound containing azabicyclohexane, and its human and mouse protein binding abilities were both less than 80%. We next synthesized compound **20**, which contained an aminomethyl group introduced into the imidazole adjacent position of compound **19** (**TP0586532**), but the antibacterial activity of this compound was attenuated, especially

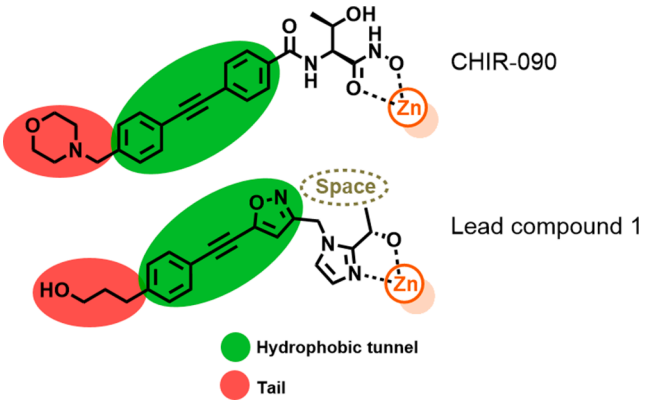

Fig. 2. Schematic structures of CHIR-090 and lead compound **1**.

against *K. pneumoniae*, from 4 μg/mL to 16 μg/mL. From among the compounds that had been obtained, compounds that were expected to have an *in vivo* efficacy were selected and further narrowed down using a murine systemic infection model (data not shown). Then, the compounds were evaluated in a murine lung infection model (*K. pneumoniae* ATCC BAA-2343, a carbapenem-resistant strain), which is a more clinically oriented *in vivo* evaluation system. The changes in the number of viable bacteria in the lung at a dose of 50 mg/kg were determined; as a result, a decrease of 1 log or more was confirmed for all the evaluated compounds in Table 3. Furthermore, the murine maximum tolerated dose (MTD) test was performed using intravenous administrations to identify compounds with a tolerable dose of 200 mg/kg. From the above results, four compounds were selected as promising drug candidates: compounds **15**, **17**, **18**, and **19** (**TP0586532**).

2.4. Cardiovascular study

Compounds **15**, **17**, **18**, and **19** (**TP0586532**) were subjected to a safety pharmacology test using the guinea pig cardiovascular system under anesthesia to further narrow down the compounds. The administration of compounds **15**, **17**, and **18**, all of which had an aminomethyl

Table 1
Exploration of tails and part A components.

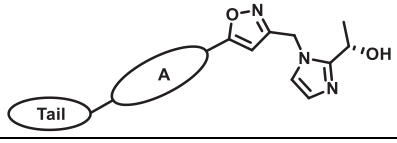

Cpd	Tail	A	LpxC IC_{50} (μM)[a]	Ec MIC[b] (μg/mL)	Kp[c] MIC (μg/mL)	PB[d] (%) Human Mouse
1 (Lead)	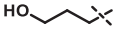	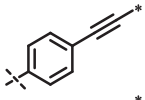	0.031	0.5	2	>99.5 >99.5
2	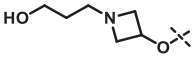	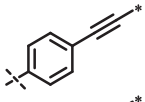	0.378	2	8	73.9 83.5
3	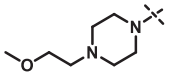	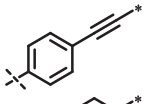	0.071	0.25	0.5	91.0 91.7
4	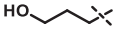	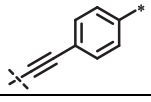	0.051	1	2	96.9 95.1

[a] Fluorescamine method.
[b] *E. coli* ATCC 25922, MIC: minimum inhibitory concentration.
[c] *K. pneumoniae* ATCC 13883.
[d] Serum protein binding.

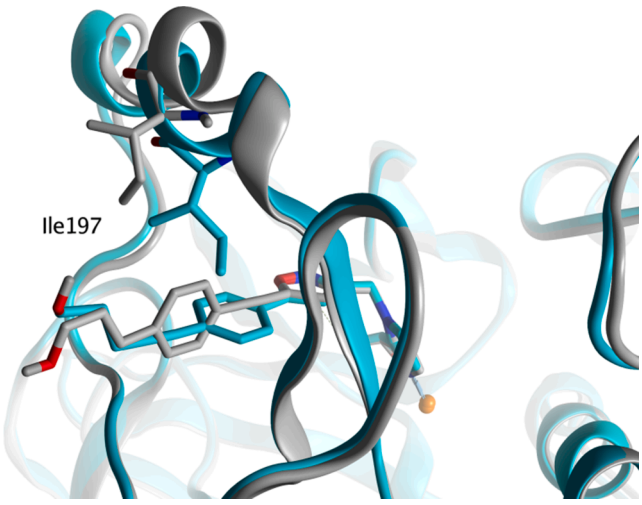

Fig. 3. Structural superposition of **4** (cyan carbons) and **5** (gray carbons) using MOE software.[25] X-ray cocrystal structures of **4** and **5** in *Pseudomonas aeruginosa* LpxC are shown (PDB ID: 7DEM and 7DEL). The key residue (Ile197) is represented in stick format. The catalytic zinc is shown as an orange sphere. The homology of the amino acid residues located in the hydrophobic tunnel region is highly retained between *P. aeruginosa*, *E. coli*, and *K. pneumoniae*.[26]

group adjacent to imidazole, induced QT prolongation and reduced both the heart rate and the blood pressure of the guinea pigs. The effects were especially strong for compounds **17** and **18** containing azabicyclohexane. On the other hand, compound **19** (**TP0586532**), which did not have an aminomethyl group, produced no remarkable changes in cardiac parameters (Fig. 4 and Table 4). The effect on QTc was consistent with the results of the hERG channel assay, in which compound **19** (**TP0586532**) showed the weakest activity (IC_{50} >1000 μM) among these four compounds. The intravenous infusion of ACHN-975, an LpxC inhibitor, at a dose of 75 mg/kg in a phase 1 clinical trial reportedly induced a marked decrease in systolic blood pressure with an increase in exposure in a cardiovascular safety test using anesthetized rats.[27] By contrast, although a rat model was not used, a decrease in blood pressure was not observed even after the administration of **TP0586532** at a dose of 150 mg/kg in an anesthetized guinea pig model. These results suggest that the cardiovascular risk of **TP0586532** is significantly less than that of ACHN-975, although the test conditions differed. Based on the results that had been obtained, compound **19** (**TP0586532**) was selected as the best compound with a low cardiovascular risk.

2.5. Safety profile of TP0586532

Next, genotoxicity tests were performed to further evaluate the safety of **TP0586532**. Both a mouse lymphoma assay and an *in vivo* micronucleus test were negative. Furthermore, a 4-day repeated dose study in rats and a 14-day repeated dose study in monkeys showed that the MTDs were 400 mg/kg (SD rat) and 400 mg/kg or more (cynomolgus monkey), respectively.

2.6. X-ray analysis of TP0586532

A cocrystal of **TP0586532** and *P. aeruginosa* LpxC is shown in Fig. 5. **TP0586532** is chelated with a zinc atom in the same manner as the 2-(1*S*-hydroxymethyl)-imidazole derivative that was shown in Fig. 3, and the nitrogen atom of azabicyclohexane creates a water-bridged hydrogen bond with the main chain of Val211. Moreover, the condensed ring of this azabicyclohexane is located along the wall of the

Table 2
Exploration of tails and part B components.

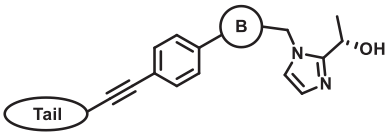

Cpd	Tail	B	LpxC IC_{50} (μM)	Ec[a] MIC (μg/mL)	Kp[b] MIC (μg/mL)	PB[c] (%) Human Mouse	Systemic infection (%)[d]
6		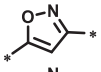	0.046[e]	0.5	1	93.0 90.1	67
7		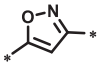	0.049[e]	0.25	0.5	97.3 96.6	0
8		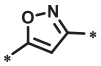	0.015[f]	0.12	0.25	98.3 96.5	0
9[g]	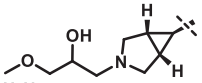	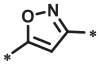	0.071[f]	0.5	0.5	93.5 91.8	33
10		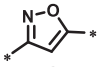	0.193[e]	1	4	88.5 85.0	NT[h]
11		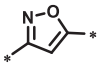	0.065[e]	0.5	2	96.5 93.1	NT
12[g]	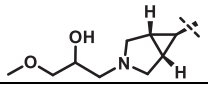	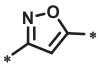	0.097[f]	0.5	0.5	92.4 92.3	17

[a] *E. coli* ATCC 25922.
[b] *K. pneumoniae* ATCC 13883.
[c] Serum protein binding.
[d] Murine systemic infection model: survival rate at day 7, *K. pneumoniae* 4102, dose: 25 mg/kg.
[e] LCMS method.
[f] Fluorescamine method.
[g] Mixture of diastereomers at the tail moiety.
[h] Not tested.

Table 3
Exploration of tails and part R components.

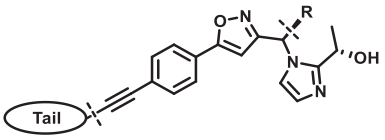

Cpd	Tail	R	LpxC IC_{50} (μM)	Ec[a] MIC (μg/mL)	Kp[b] MIC (μg/mL)	PB[c] (%) Human Mouse	Lung infection (log_{10}CFU/lung)[d]	Mouse MTD (mg/kg)[e]
13			0.282[f]	2	8	NT[h] NT	NT	NT
14	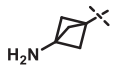		0.279[f]	0.5	2	89.7 91.6	−2.48	100
15	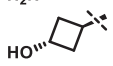		<0.037[f]	0.25	1	92.6 93.0	−1.99	≥200
16	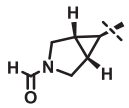		0.039 [g]	1	2	90.5 91.0	−2.84	100
17	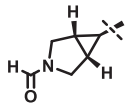		ND[i]	1	2	72.5 82.0	−2.47	≥200
18	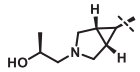		NT	1	4	78.8 84.9	−1.19	≥200
19 (TP0586532)	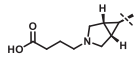		0.101[g]	2	4	77.7 75.9	−1.63	≥200
20	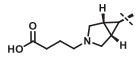		NT	4	16	NT NT	NT	NT

[a] *E. coli* ATCC 25922.
[b] *K. pneumoniae* ATCC 13883.
[c] Serum protein binding.
[d] Murine lung infection model: means of logarithm changes in the bacterial burden in the lung relative to the start of therapy (n = 5), *K. pneumoniae* ATCC BAA-2343, dose: 50 mg/kg.
[e] Maximum tolerated dose during single intravenous administration, ICR mouse (n = 2).
[f] LCMS method.
[g] Fluorescamine method.
[h] Not tested.
[i] Not determined.

tail-side exit of the hydrophobic tunnel, indicating the superiority of this characteristic tail type.

3. Chemistry

The synthesis of compounds **1**–**20** is depicted in Schemes 1–4. Key intermediate **21** was coupled to aryl iodide **24** using a Sonogashira coupling reaction to yield compound **2**. Piperazine derivative **3** was prepared from compound **23** using a palladium-catalyzed Buchwald-Hartwig amination (Scheme 1).

Isoxazole-phenyl-ethynyl type compounds **4**, **6–8**, and intermediate **37** were prepared from aryl iodide **25** or **26** using a Suzuki-Miyaura coupling reaction or Sonogashira coupling. Azabicyclo[3.1.0]hexane derivative **37** led to the creation of the elongated compounds **9**, **16**, and **19** according to their respective methods (Scheme 2).

Different isoxazole compounds **10**–**12** were synthesized from aryl iodide **40** using procedures similar to those used for compounds **4**–**9** in Scheme 2 (Scheme 3).

The aminomethyl branch compounds **13**–**15** were synthesized from aryl iodide intermediate **45** or **46** containing an *N*-Boc protected aminomethyl branch. In addition, compounds **17**, **18**, and **20** were prepared by procedures similar to those used for compounds **16**, **9**, and **19** in Scheme 2, respectively (Scheme 4).

4. Conclusion

We conducted lead optimization starting from a non-hydroxamate lead compound **1** with the aim of creating a novel LpxC inhibitor. The use of protein binding as an index was useful for guiding improvements in the *in vivo* efficacy while maintaining the antibacterial activity. Structural transformation was performed from the tail site to the adjacent position of the imidazole, and promising compounds were identified using cardiovascular studies in anesthetized guinea pigs. These efforts resulted in the introduction of a carboxy group at the tail site, rather than the introduction of a primary amine to the adjacent position of the imidazole. Finally, we identified **TP0586532** as a compound with a low cardiovascular risk that was effective against *K. pneumoniae*, including resistant strains. Further detailed evaluations and results will be reported in due course.

5. Experimental section

5.1. Chemistry

All reagents and solvents were of commercial quality and were used without further purification. The progress of the reactions was usually monitored using thin-layer chromatography (TLC; Merck silica gel 60 F_{254} plates or Fuji Silysia chromatorex NH plates). Purifications using silica gel column chromatography were performed using a Biotage

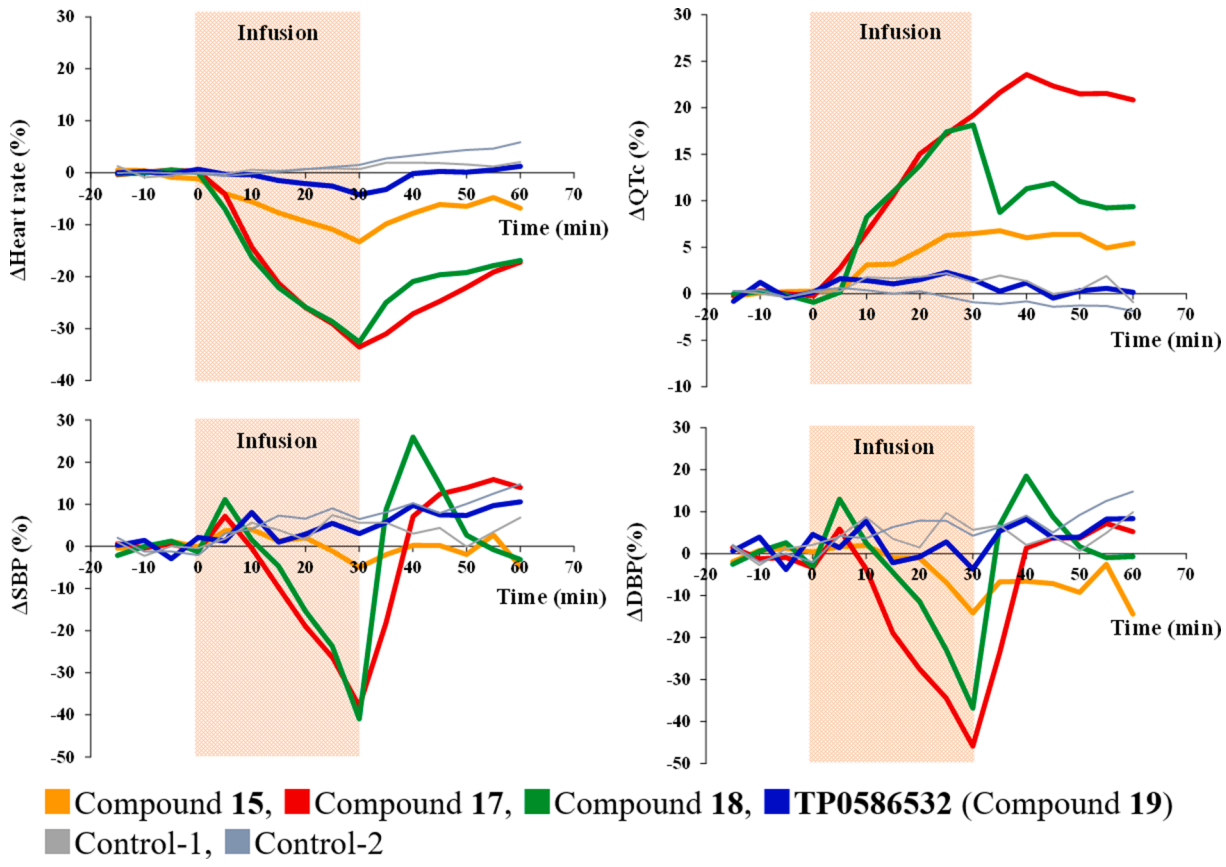

Fig. 4. Safety pharmacology study examining the effects of test compounds on the cardiovascular system in anesthetized guinea pigs. SBP: systolic blood pressure. DBP: diastolic blood pressure.

Table 4
Toxicokinetic parameters affecting the cardiovascular system in anesthetized guinea pigs.

Cpd	15	17	18	19 (TP0586532)
Dose (mg/kg/30 min)	60	180	135	150
f_u [a,b]	0.172	0.255	0.273	0.231
C_{30min} (μg/mL)[c]	90.7	233	132	378
C_{30min_free} (μg/mL)[d]	15.6	59.4	36.0	87.3

[a] f_u: fraction unbound in plasma, assumed to be equal to the fraction unbound in serum.
[b] The protein binding assay was evaluated at a concentration of 500 μg/mL in guinea pig serum.
[c] Plasma concentration at the end of infusion.
[d] Unbound plasma concentration at the end of infusion.

Isolera One instrument with Biotage SNAP Ultra Cartridges (particle size: 25 μm sphere), BÜCHI Reveleris Flash Cartridges (particle size: 40 μm), or Biotage SNAP Isolute NH_2 Cartridges (particle size: 50 μm). ^1H NMR spectra were recorded at 400 MHz using a BRUKER AVANCE III HD 400 spectrometer or 600 MHz using a JEOL ECA600 spectrometer with tetramethylsilane (TMS) as the internal standard, and proton chemical shifts were expressed in parts per million (ppm) in the indicated solvent. Multiplicity was defined as s (singlet), d (doublet), t (triplet), q (quartet), quin (quintet), dd (double doublet), m (multiplet), or br (broad signal). ^{13}C NMR spectra were recorded at 125 MHz using a JEOL ECA500 spectrometer with TMS as the internal standard, and carbon chemical shifts were expressed in parts per million (ppm) in DMSO-d_6 solvent. High-resolution mass spectrometry (HRMS) findings were recorded using a Shimadzu LCMS-IT-TOF mass spectrometer with an electrospray ionization (ESI)/atmospheric pressure chemical ionization (APCI) dual source. Microwave irradiation experiments were performed using a Biotage Initiator$^+$ 60EXP with standard Pyrex vessels (capacity, 2–20 mL). The high-performance liquid chromatography mass spectra (LCMS) and retention times (Rt) were measured under the following conditions (Analytical conditions A–B).

Analytical condition A

Measuring instruments: Agilent 1290 Infinity and Agilent 6130 or 6150 of Agilent, with Agilent 385-ELSD being used in combination with an ELSD detector as an attachment. Column: Acquity CSH C18, 1.7 μm, 2.1 × 50 mm (Waters). Ionization method: ESI. Solvents: Fluid A, 0.1% formic acid-containing water; Fluid B, 0.1% formic acid containing acetonitrile. Flow rate: 0.8 mL/min.

Detection method: 210 nm and 254 nm. Gradients: 0.0–0.8 min (Fluid A/Fluid B = 95/5–60/40), 0.8–1.08 min (Fluid A/Fluid B = 60/40–1/99), 1.08–1.38 min (Fluid A/Fluid B = 1/99).

Analytical condition B

The measuring instruments, column, ionization method, solvents, flow rate, and detection method were the same as those used for Analytical condition A. Gradients: 0.0–1.2 min (Fluid A/Fluid B = 80/20–1/99), 1.2–1.4 min (Fluid A/Fluid B = 1/99).

*5.1.1. 3-[3-(4-{[3-({2-[(1S)-1-Hydroxyethyl]-1H-imidazol-1-yl}methyl)-1,2-oxazol-5-yl]ethynyl}phenoxy)azetidin-1-yl]propan-1-ol (**2**)*

A mixture of 5-ethynyl-3-[(2-{(1*S*)-1-[(oxan-2-yl)oxy]ethyl}-1*H*-imidazol-1-yl)methyl]-1,2-oxazole **21** (59 mg, 0.20 mmol), 1-(3-{[*tert*-butyl(dimethyl)silyl]oxy}propyl)-3-(4-iodophenoxy)azetidine **24** (see supplementary data, 80 mg, 0.18 mmol), $Pd(PPh_3)_2Cl_2$ (6.3 mg, 0.0089 mmol), CuI (1.0 mg, 0.0054 mmol), and Et_3N (0.25 mL, 1.8 mmol) in

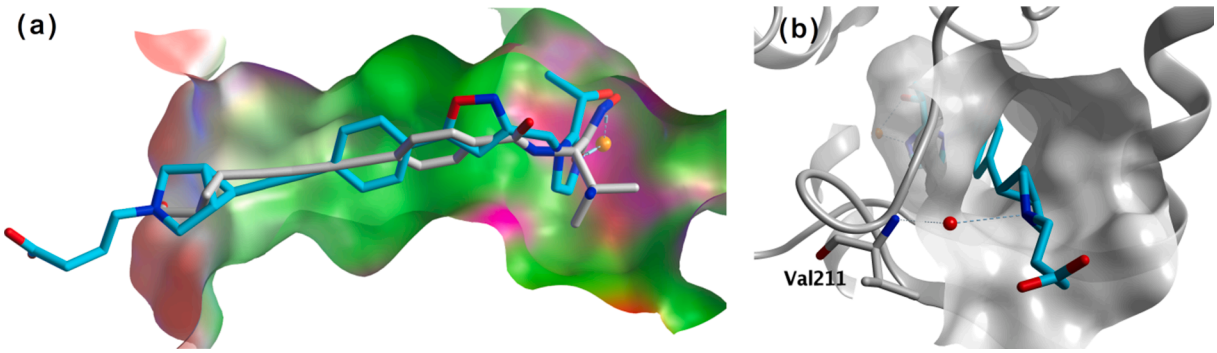

Fig. 5. (a) Overlap of **TP0586532** (cyan carbons, PDB ID: 7DEN) and **ACHN-975** (gray carbons, PDB ID: 6MOO) bound to *P. aeruginosa* LpxC. The residues on the surface are colored as follows: lipophilic reagions are in light green, hydrophilic in pink, and exposed in red. The catalytic zinc is displayed as an orange sphere. (b) View of **TP0586532** (cyan carbons) from the tail side. Val211 is represented in stick format. A water molecule is displayed as a red ball. The relevant interactions are indicated by the dashed lines.

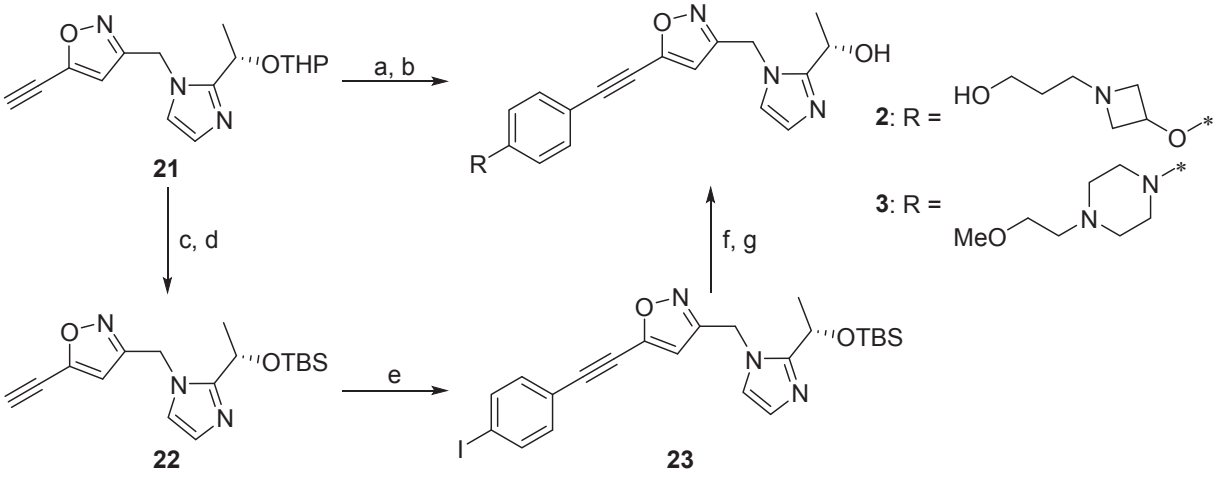

Scheme 1. Synthesis of isoxazole-ethynyl-phenyl type compounds 2 and 3. Reagents and conditions: (a) 1-(3-{[*tert*-butyl(dimethyl)silyl]oxy}propyl)-3-(4-iodophenoxy)azetidine **24** (see supplementary data), $Pd(PPh_3)_2Cl_2$, CuI, Et_3N, DMF, 60 °C, 1 h; (b) $TsOH{\cdot}H_2O$, MeOH, rt, 16 h, 40% over two steps; (c) $TsOH{\cdot}H_2O$, MeOH, rt, 2 h; (d) TBSCl, imidazole, DMF, rt, 3 h, 80% over two steps; (e) 1,4-diiodobenzene, $Pd(PPh_3)_4$, CuI, Et_3N, MeCN, rt, 1 h, 61%; (f) 1-(2-methoxyethyl) piperazine, $Pd_2(dba)_3$, 2-dicyclohexylphosphino-2′-(*N*,*N*-dimethylamino)biphenyl, *tert*-BuONa, toluene, 60 °C, 5.5 h, 76%; (g) 1 mol/L TBAF in THF, THF, rt, 0.5 h, 80%.

DMF (0.51 mL) was stirred at 60 °C for 1 h. The mixture was diluted with $CHCl_3$. The insoluble matter was removed by filtration, and the filtrate was concentrated. The residue was dissolved in MeOH followed by the addition of $TsOH{\cdot}H_2O$ (136 mg, 0.72 mmol). After stirring for 16 h, the reaction mixture was poured into aqueous saturated $NaHCO_3$, and the mixture was extracted twice with 5% MeOH in $CHCl_3$. The combined organic layer was dried over $MgSO_4$, filtered, and concentrated. The residue was purified using column chromatography on NH silica gel and eluted with MeOH/$CHCl_3$ to obtain **2** as a colorless solid (30 mg, 40% over two steps). ^{1}H NMR (600 MHz, DMSO-d_6) δ 7.59–7.55 (m, 2H), 7.16 (d, J = 1.2 Hz, 1H), 6.95–6.91 (m, 2H), 6.82 (s, 1H), 6.80 (s, 1H), 5.46–5.39 (m, 3H), 4.87–4.82 (m, 2H), 4.39 (t, J = 5.0 Hz, 1H), 3.75–3.69 (m, 2H), 3.44–3.38 (m, 2H), 2.97–2.90 (m, 2H), 2.48–2.44 (m, 2H), 1.47–1.41 (m, 5H). ^{13}C NMR (125 MHz, DMSO-d_6) δ 161.6, 158.4, 152.9, 149.7, 133.7, 126.5, 120.9, 115.3, 111.8, 107.6, 98.8, 74.2, 66.6, 61.4, 60.5, 58.9, 56.3, 40.5, 30.6, 21.8. LCMS (ESI) m/z 423 $[M+H]^+$. Rt 0.527 min (Analytical condition A). HRMS (ESI/APCI dual) m/z calcd for $C_{23}H_{26}N_4O_4$ $[M+H]^+$ 423.2027, found 423.2020.

5.1.2. (1S)-1-(1-{[5-({4-[4-(2-Methoxyethyl)piperazin-1-yl]phenyl} ethynyl)-1,2-oxazol-3-yl]methyl}-1H-imidazol-2-yl)ethan-1-ol (3)

In step 1, sodium *tert*-butoxide (18 mg, 0.19 mmol) was added to a solution of 3-({2-[(1*S*)-1-{[*tert*-butyl(dimethyl)silyl]oxy}ethyl]-1*H*-imidazol-1-yl}methyl)-5-[(4-iodophenyl)ethynyl]-1,2-oxazole **23** (50 mg, 0.094 mmol), 1-(2-methoxyethyl)piperazine (27 mg, 0.19 mmol), $Pd_2(dba)_3$ (4.3 mg, 0.0047 mmol), and 2-dicyclohexylphosphino-2′-(*N*,*N*-dimethylamino)biphenyl (3.7 mg, 0.0094 mmol) in toluene (1 mL). The mixture was stirred at 60 °C for 5.5 h. After cooling, the mixture was diluted with aqueous $NaHCO_3$ and extracted with $CHCl_3$. The organic layer was dried over $MgSO_4$ and concentrated. The residue was purified using column chromatography on NH silica gel and eluted with EtOAc/*n*-hexane to obtain 1-(4-{[3-({2-[(1*S*)-1-{[*tert*-butyl (dimethyl)silyl]oxy}ethyl]-1*H*-imidazol-1-yl}methyl)-1,2-oxazol-5-yl] ethynyl}phenyl)-4-(2-methoxyethyl)piperazine as a pale yellow amorphous substance (39 mg, 76%). LCMS (ESI) m/z 550 $[M+H]^+$. Rt 0.597 min (Analytical condition B).

In step 2, 1 mol/L TBAF in THF (0.089 mL, 0.089 mmol) was added to a solution of the above-described amorphous substance (38 mg, 0.069 mmol) in THF (0.7 mL). The mixture was stirred at room temperature for 0.5 h, quenched with 20% aqueous potassium carbonate, and extracted with 10% MeOH in $CHCl_3$. The organic extract was passed through a phase separator and concentrated. The residue was purified using column chromatography on NH silica gel and eluted with EtOAc/*n*-hexane and MeOH/$CHCl_3$ to obtain **3** as a pale yellow solid (24 mg, 80%). ^{1}H NMR (400 MHz, DMSO-d_6) δ 7.44 (d, J = 8.7 Hz, 2H), 7.16 (d, J = 0.8 Hz, 1H), 6.97 (d, J = 8.7 Hz, 2H), 6.81 (d, J = 0.8 Hz, 1H), 6.72

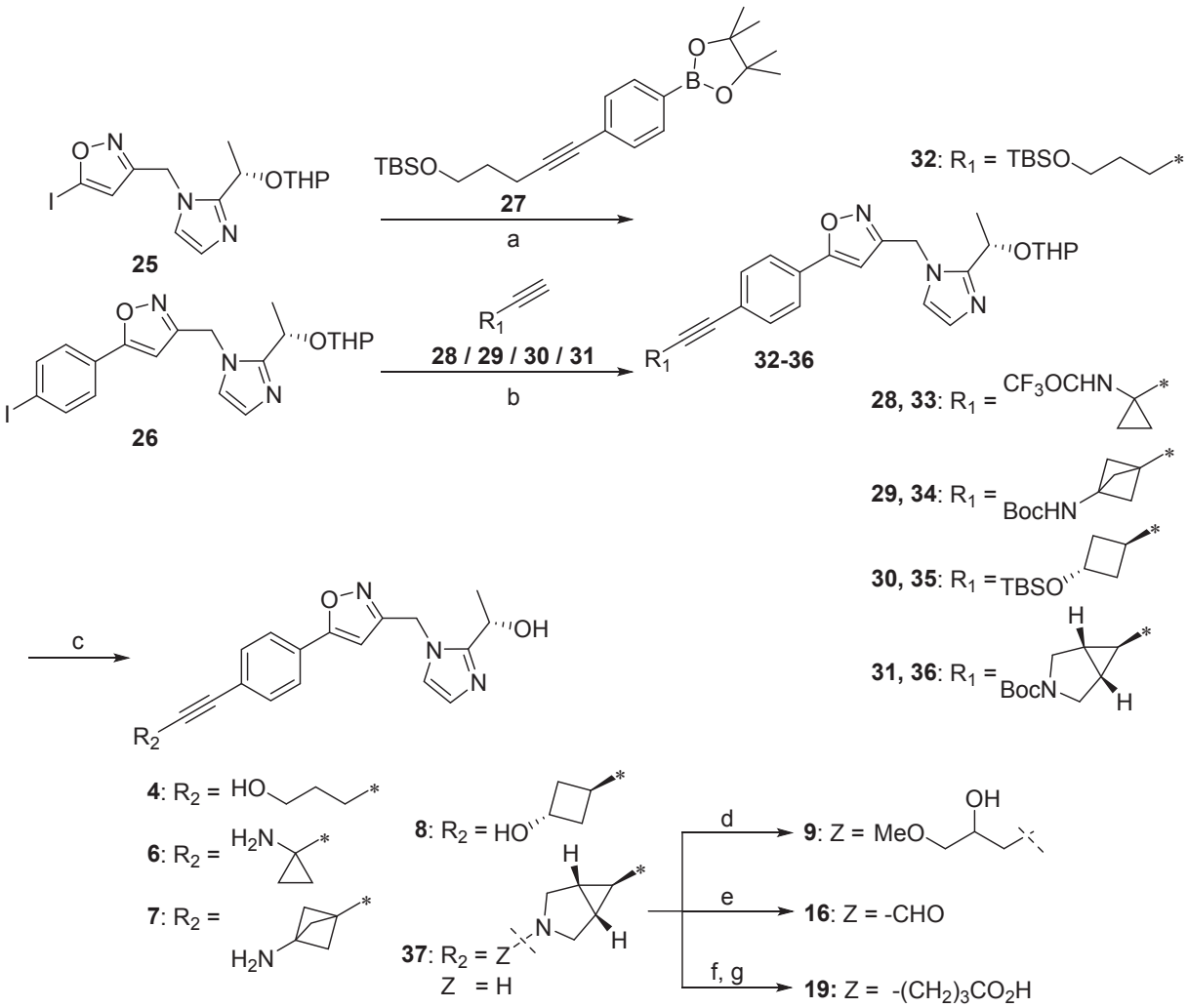

Scheme 2. Synthesis of isoxazole-phenyl-ethynyl type compounds 4, 6–9, 16, and 19. Reagents and conditions: (a) **27** (see supplementary data), $Pd(PPh_3)_4$, Na_2CO_3, toluene, EtOH, 80 °C, 4 h; (b) **28**, **29**, **30** (see supplementary data) or **31** (see supplementary data), Superstable Pd(0), CuI, Et_3N, MeCN, rt, 1–2.5 h, 81%–97%; (c) **4**: **32**, TsOH·H_2O, MeOH, rt, 16 h, 19% over two steps; **6**: i) **33**, K_2CO_3, MeOH, rt, 8 h, 95%; ii) TsOH·H_2O, MeOH, rt, 2 h, 99%; **7**: **34**, TFA, $CHCl_3$, 0 °C, 4 h, 87%; **8**: **35**, 4 mol/L HCl in 1,4-dioxane, 1,4-dioxane, rt, 2 h, 72%; **37**: **36**, 4 mol/L HCl in 1,4-dioxane, 1,4-dioxane, MeOH, rt, 100 min, 60%; (d) **37**, 2-(methoxymethyl)oxirane, MeOH, 50 °C, 1.5 h, microwave, 82%; (e) *N*-formylsaccharin, THF, DMF, rt, 1 h, 70%; (f) ethyl 4-bromobutanoate, K_2CO_3, NaI, DMF, 80 °C, 80 min, 75%; (g) 2 mol/L NaOH, MeOH, THF, rt, 2 h, 77%. Superstable Pd = tris{tris[3,5-bis(trifluoromethyl)phenyl]phosphine}palladium.

(s, 1H), 5.45–5.35 (m, 3H), 4.90–4.80 (m, 1H), 3.46 (t, $J = 5.7$ Hz, 2H), 3.29–3.21 (m, 6H), 2.57–2.49 (m, 7H), 1.46 (d, $J = 6.5$ Hz, 3H). ^{13}C NMR (125 MHz, DMSO-d_6) δ 161.5, 153.3, 151.8, 149.7, 133.0, 126.5, 120.9, 114.2, 107.5, 106.9, 100.2, 73.8, 70.0, 61.4, 58.0, 56.9, 52.8, 46.7, 40.5, 21.8. LCMS (ESI) *m/z* 436 $[M+H]^+$. Rt 0.570 min (Analytical condition A). HRMS (ESI/APCI dual) *m/z* calcd for $C_{24}H_{29}N_5O_3$ $[M+H]^+$ 436.2343, found 436.2326.

5.1.3. 5-{4-[3-({2-[(1S)-1-Hydroxyethyl]-1H-imidazol-1-yl}methyl)-1,2-oxazol-5-yl]phenyl}pent-4-yn-1-ol (4)

A mixture of 5-iodo-3-[(2-{(1*S*)-1-[(oxan-2-yl)oxy]ethyl}-1*H*-imidazol-1-yl)methyl]-1,2-oxazole **25** (90 mg, 0.22 mmol), *tert*-butyl (dimethyl)({5-[4-(4,4,5,5-tetramethyl-1,3,2-dioxaborolan-2-yl)phenyl] pent-4-yn-1-yl}oxy)silane **27** (107 mg, 0.27 mmol), $Pd(PPh_3)_4$ (26 mg, 0.022 mmol), and 2 mol/L aqueous Na_2CO_3 (0.22 mL, 0.44 mmol) in toluene (0.45 mL) and EtOH (0.22 mL) was stirred at 80 °C for 2 h, followed by the addition of $Pd(PPh_3)_4$ (26 mg, 0.022 mmol) and additional stirring at 80 °C for 2 h. After cooling, the mixture was poured into ice water and extracted with EtOAc twice. The combined organic extracts were washed with brine, dried over $MgSO_4$ and concentrated. The residue was purified using column chromatography on silica gel and eluted with MeOH/$CHCl_3$ to obtain the crude product of 5-[4-(5-{[*tert*-butyl(dimethyl)silyl]oxy}pent-1-yn-1-yl)phenyl]-3-[(2-{(1*S*)-1-[(oxan-2-yl)oxy]ethyl}-1*H*-imidazol-1-yl)methyl]-1,2-oxazole **32**, which was dissolved in MeOH (1.1 mL); TsOH·H_2O (106 mg, 0.56 mmol) was then added. The mixture was stirred for 16 h. The mixture was poured into saturated aqueous $NaHCO_3$ and extracted with 5% MeOH in $CHCl_3$ twice. The combined organic extracts were dried over $MgSO_4$ and concentrated. The residue was purified using column chromatography on NH silica gel and eluted with MeOH/EtOAc to obtain **4** as a pale yellow oil (15 mg, 19% over two steps). ^1H NMR (600 MHz, CHLOROFORM-*d*) δ 7.65 (d, $J = 8.3$ Hz, 2H), 7.46 (d, $J = 8.3$ Hz, 2H), 7.02 (d, $J = 1.2$ Hz, 1H), 6.97 (d, $J = 1.2$ Hz, 1H), 6.35 (s, 1H), 5.28–5.41 (dd, $J = 15.7$, 15.7, 2H), 5.06–5.00 (m, 1H), 3.85–3.80 (m, 2H), 2.57 (t, $J = 6.6$ Hz, 2H), 2.37 (d, $J = 6.6$ Hz, 1H), 1.88 (quin, $J = 6.6$ Hz, 2H), 1.70 (d, $J = 6.6$ Hz, 3H). ^{13}C NMR (125 MHz, DMSO-d_6) δ 168.8, 161.7, 149.7, 132.0, 126.2, 125.7, 125.6, 125.3, 121.0, 100.1, 93.2, 79.9, 61.3, 59.4, 40.7, 31.4, 21.8, 15.4. LCMS (ESI) *m/z* 352 $[M+H]^+$. Rt 0.830 min (Analytical condition A). HRMS (ESI/APCI dual) *m/z* calcd for $C_{20}H_{21}N_3O_3$ $[M+H]^+$ 352.1656, found 352.1650.

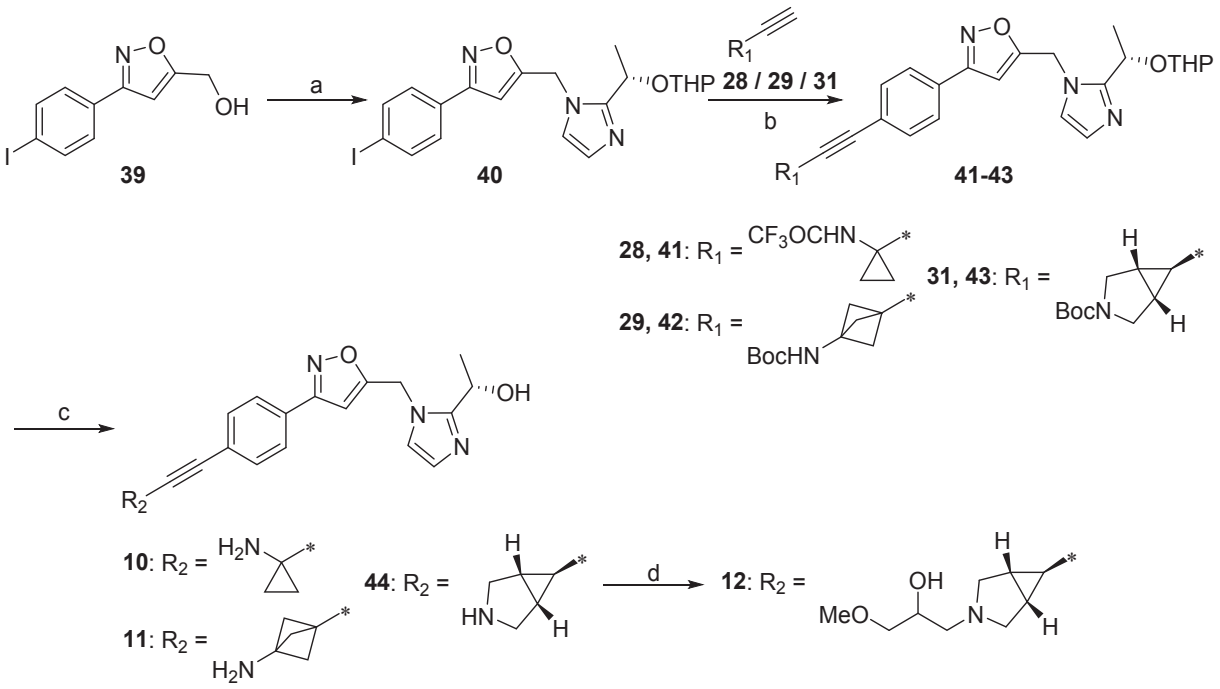

Scheme 3. Synthesis of isoxazole-phenyl-ethynyl type compounds 10–12. Reagents and conditions: (a) 2-{(1*S*)-1-[(oxan-2-yl)oxy]ethyl}-1*H*-imidazole, TMAD, Bu_3P, THF, rt, 22 h, 65%; (b) **41**, **42**: **28** or **29**, $Pd(PPh_3)_4$, CuI, Et_3N, DMF, 65 °C, 0.5–1 h; **43**: **31**, Superstable Pd(0), CuI, Et_3N, MeCN, rt–55 °C, 1.5 h, 92%; (c) **10**: i) **41**, 2 mol/L HCl in MeOH, MeOH, 0 °C–rt, 1.5 h; ii) 1 mol/L NaOH, MeOH, rt, 16 h, 81% over three steps; **11**: **42**, TFA, $CHCl_3$, 0 °C–rt, 2 h, 88% over two steps; **12**: **43**, 4 mol/L HCl in 1,4-dioxane, rt, 3.5 h, 99%; (d) 2-(methoxymethyl)oxirane, EtOH, MeOH, 60 °C, 1 h, 75%.

5.1.4. (1S)-1-{1-[(5-{4-[(1-Aminocyclopropyl)ethynyl]phenyl}-1,2-oxazol-3-yl)methyl]-1H-imidazol-2-yl}ethan-1-ol (6)

In step 1, a 20% aqueous K_2CO_3 (5.4 g) solution was added to a solution of 2,2,2-trifluoro-*N*-{1-[(4-{3-[(2-{(1*S*)-1-[(oxan-2-yl)oxy]ethyl}-1*H*-imidazol-1-yl)methyl]-1,2-oxazol-5-yl}phenyl)ethynyl]cyclopropyl}acetamide **33** (683 mg, 1.29 mmol) in MeOH (25 mL), and the mixture was stirred at room temperature for 4 h. Additional 20% aqueous K_2CO_3 (5.4 g) solution was then added at that temperature. After stirring at the same temperature for 4 h, water was added to the mixture, which was then extracted with $CHCl_3$. The organic extract was passed through a phase separator and concentrated. The residue was purified using column chromatography on NH silica gel and eluted with MeOH/$CHCl_3$ to obtain 1-[(4-{3-[(2-{(1*S*)-1-[(oxan-2-yl)oxy]ethyl}-1*H*-imidazol-1-yl)methyl]-1,2-oxazol-5-yl}phenyl)ethynyl]cyclopropan-1-amine as a pale yellow syrup (529 mg, 95%). LCMS (ESI) *m/z* 433 $[M+H]^+$. Rt 0.686 min (Analytical condition A).

In step 2, TsOH·H_2O (647 mg, 3.40 mmol) was added to a solution of the above-described product (368 mg, 0.85 mmol) in MeOH (8.5 mL). After stirring at room temperature for 2 h, 20% aqueous K_2CO_3 solution was added to the mixture, which was extracted with $CHCl_3$. The organic extract was passed through a phase separator and concentrated. The residue was purified using column chromatography on NH silica gel and eluted with MeOH/$CHCl_3$ to obtain **6** as a colorless amorphous substance (292 mg, 99%). ^{1}H NMR (600 MHz, CHLOROFORM-*d*) δ 7.65 (d, $J = 8.3$ Hz, 2H), 7.44 (d, $J = 8.3$ Hz, 2H), 7.01 (d, $J = 1.2$ Hz, 1H), 6.96 (d, $J = 1.2$ Hz, 1H), 6.36 (s, 1H), 5.41–5.37 (m, 1H), 5.33–5.28 (m, 1H), 5.06–4.99 (m, 1H), 1.69 (d, $J = 6.6$ Hz, 3H), 1.08–1.00 (m, 4H). ^{13}C NMR (125 MHz, DMSO-d_6) δ 168.8, 161.8, 149.7, 131.8, 126.5, 125.7, 125.5, 125.2, 120.9, 100.1, 98.9, 77.1, 61.4, 40.7, 24.5, 21.8, 18.1. LCMS (ESI) *m/z* 349 $[M+H]^+$. Rt 0.484 min (Analytical condition A). HRMS (ESI/APCI dual) *m/z* calcd for $C_{20}H_{20}N_4O_2$ $[M+H]^+$ 349.1659, found 349.1671.

5.1.5. (1S)-1-{1-[(5-{4-[(3-Aminobicyclo[1.1.1]pentan-1-yl)ethynyl]phenyl}-1,2-oxazol-3-yl)methyl]-1H-imidazol-2-yl}ethan-1-ol (7)

TFA (0.096 mL, 1.3 mmol) was added to a solution of *tert*-butyl {3-[(4-{3-[(2-{(1*S*)-1-[(oxan-2-yl)oxy]ethyl}-1*H*-imidazol-1-yl)methyl]-1,2-oxazol-5-yl}phenyl)ethynyl]bicyclo[1.1.1]pentan-1-yl}carbamate **34** (70 mg, 0.13 mmol) in $CHCl_3$ (0.42 mL) at 0 °C. After stirring for 2 h, additional TFA (0.096 mL, 1.3 mmol) was added. The mixture was stirred at 0 °C for another 2 h and quenched by adding MeOH, then concentrated. The residue was partitioned between 10% MeOH in $CHCl_3$ and 2 mol/L Na_2CO_3. The aqueous layer was extracted three times with 10% MeOH in $CHCl_3$. The combined organic extracts were dried over $MgSO_4$ and concentrated. The residue was purified using column chromatography on NH silica gel and eluted with MeOH/$CHCl_3$ to obtain **7** as a colorless amorphous substance (41 mg, 87%). ^{1}H NMR (400 MHz, METHANOL-d_4) δ 7.74 (d, $J = 8.4$ Hz, 2H), 7.46 (d, $J = 8.4$ Hz, 2H), 7.15 (d, $J = 1.1$ Hz, 1H), 6.92 (d, $J = 1.1$ Hz, 1H), 6.72 (s, 1H), 5.58–5.41 (m, 2H), 5.04 (q, $J = 6.6$ Hz, 1H), 2.12 (s, 6H), 1.59 (d, $J = 6.6$ Hz, 3H). ^{13}C NMR (125 MHz, DMSO-d_6) δ 168.7, 161.8, 149.7, 132.1, 126.5, 125.8, 125.7, 124.6, 120.9, 100.2, 91.3, 80.1, 61.4, 57.6, 51.6, 40.7, 23.6, 21.8. LCMS (ESI) *m/z* 375 $[M+H]^+$. Rt 0.442 min (Analytical condition A). HRMS (ESI/APCI dual) *m/z* calcd for $C_{22}H_{22}N_4O_2$ $[M+H]^+$ 375.1816, found 375.1798.

5.1.6. (1S,3r)-3-({4-[3-({2-[(1S)-1-Hydroxyethyl]-1H-imidazol-1-yl}methyl)-1,2-oxazol-5-yl]phenyl}ethynyl)cyclobutan-1-ol (8)

Four mol/L HCl in 1,4-dioxane (2.0 mL) was added to a solution of 5-(4-{[(1*r*,3*S*)-3-{[*tert*-butyl(dimethyl)silyl]oxy}cyclobutyl]ethynyl}phenyl)-3-[(2-{(1*S*)-1-[(oxan-2-yl)oxy]ethyl}-1*H*-imidazol-1-yl)methyl]-1,2-oxazole **35** (47 mg, 0.084 mmol) in 1,4-dioxane (2.0 mL). The mixture was stirred at room temperature for 2 h and concentrated. The residue was basified with saturated aqueous $NaHCO_3$ and extracted with $CHCl_3$. The organic extract was passed through a phase separator and concentrated. The residue was purified using column chromatography on NH silica gel and eluted with MeOH/$CHCl_3$ to obtain **8** as a colorless solid (22 mg, 72%). ^{1}H NMR (400 MHz,

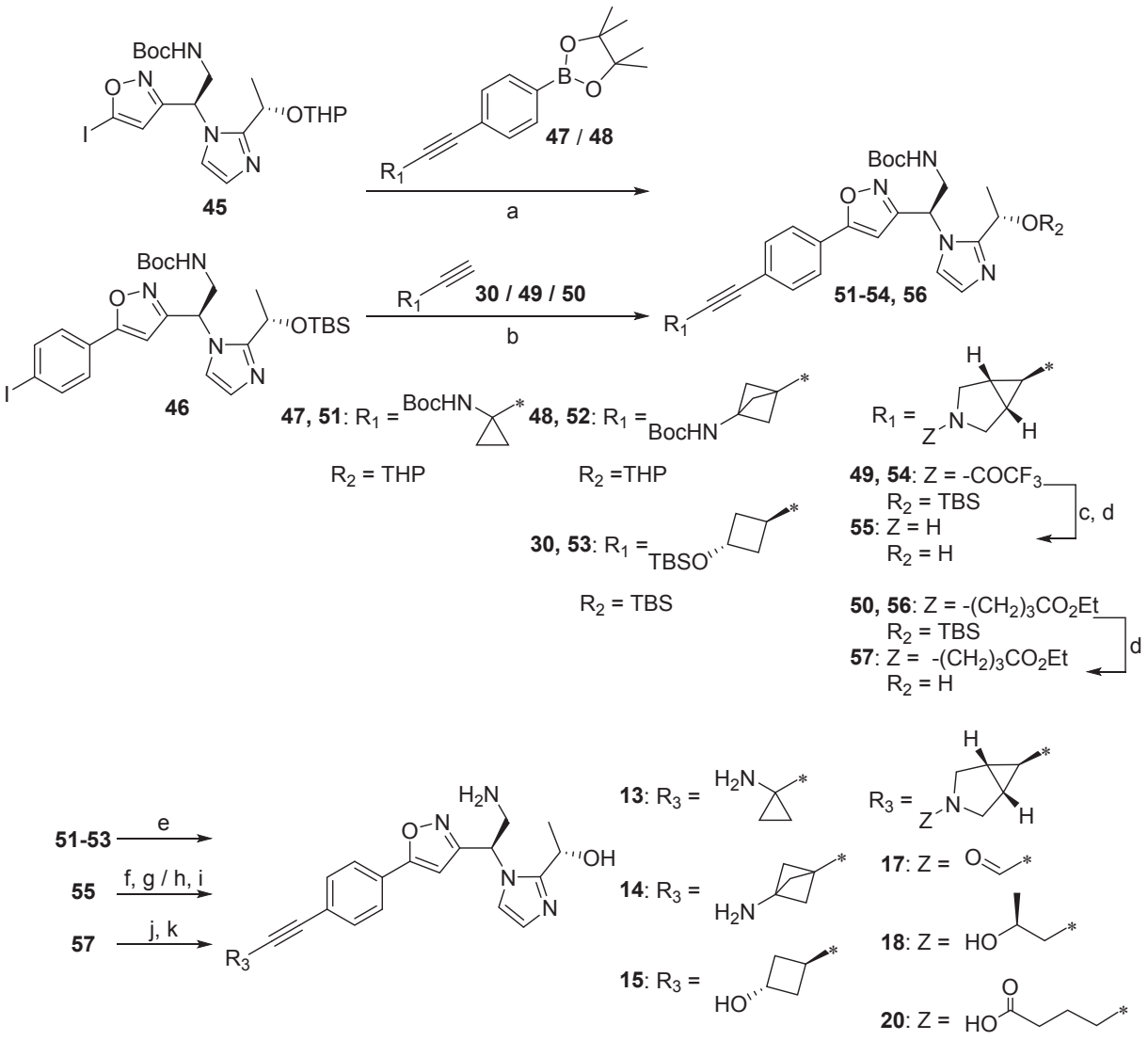

Scheme 4. Synthesis of aminomethyl branch compounds 13–15, 17, 18, and 20. Reagents and conditions: (a) **51**: **47**, Pd-PEPPSI-IPent catalyst, 2 mol/L Na_2CO_3, toluene, EtOH, 100 °C, 2 h; **52**: **48**, Pd-PEPPSI-IPent catalyst, 2 mol/L Na_2CO_3, toluene, EtOH, 80 °C, 1 h; (b) **53**: **30**, Superstable Pd(0), CuI, Et_3N, MeCN, 60 °C, 10 min, 99%; **54**: **49**, $Pd(PPh_3)_4$, CuI, Et_3N, DMF, 65 °C, 0.5 h; **56**: **50**, Superstable Pd(0), CuI, Et_3N, MeCN, rt, 2 h; 90%; (c) 1 mol/L NaOH, THF, MeOH, rt, 20 min, 77% over two steps; (d) 1 mol/L TBAF in THF, THF, rt, 20 min–1 h, 85%–95%; (e) **13**: **51**, TFA, $CHCl_3$, rt, 2 h, 20% over two steps; **14**: **52**, TFA, $CHCl_3$, MeOH, rt, 1.25 h, 31% over two steps; **15**: **53**, 4 mol/L HCl in 1,4-dioxane, MeOH, rt, 5 h, 94%; (f) **55**, *N*-formylsaccharin, THF, rt, 40 min, 89%; (g) 4 mol/L HCl in 1,4-dioxane, MeOH, rt, 1 h, 85%; (h) **55**, (2*S*)-2-methyloxirane, MeOH, 50 °C, 2.5 h, microwave; (i) 4 mol/L HCl in 1,4-dioxane, MeOH, rt, 1 h, quant over two steps; (j) **57**, 4 mol/L HCl in 1,4-dioxane, MeOH, rt, 1 h; (k) 1 mol/L NaOH, THF, rt, 2 h, 34% over two steps. Pd-PEPPSI-IPent = [1,3-bis(2,6-di-3-pentylphenyl)imidazol-2-ylidene](3-chloropyridyl)dichloropalladium(II).

CHLOROFORM-*d*) δ 7.65 (d, $J = 8.1$ Hz, 2H), 7.46 (d, $J = 8.1$ Hz, 2H), 7.02 (br s, 1H), 6.97 (br s, 1H), 6.36 (s, 1H), 5.44–5.26 (m, 2H), 5.09–4.97 (m, 1H), 4.66 (quin, $J = 6.7$ Hz, 1H), 3.28–3.18 (m, 1H), 2.57–2.46 (m, 2H), 2.38–2.26 (m, 2H), 1.69 (d, $J = 6.4$ Hz, 3H). ^{13}C NMR (125 MHz, DMSO-d_6) δ 168.8, 161.8, 149.7, 132.0, 126.5, 125.7, 125.6, 125.2, 120.9, 100.1, 97.4, 80.0, 64.4, 61.4, 40.9, 40.7, 21.8, 17.4. LCMS (ESI) *m/z* 364 $[M+H]^+$. Rt 0.460 min (Analytical condition B). HRMS (ESI/APCI dual) *m/z* calcd for $C_{21}H_{21}N_3O_3$ $[M+H]^+$ 364.1656, found 364.1642.

5.1.7. 1-[(1R,5S,6s)-6-({4-[3-({2-[(1S)-1-Hydroxyethyl]-1H-imidazol-1-yl}methyl)-1,2-oxazol-5-yl]phenyl}ethynyl)-3-azabicyclo[3.1.0]hexan-3-yl]-3-methoxypropan-2-ol (9)

2-(Methoxymethyl)oxirane (35.3 mg, 0.40 mmol) was added to a solution of (1*S*)-1-(1-{[5-(4-{[(1*R*,5*S*,6*s*)-3-azabicyclo[3.1.0]hexan-6-yl]ethynyl}phenyl)-1,2-oxazol-3-yl]methyl}-1*H*-imidazol-2-yl)ethan-1-ol **37** (30 mg, 0.080 mmol) in MeOH (1 mL). The mixture was stirred at 50 °C for 0.5 h under microwave irradiation. Additional 2-(methoxymethyl)oxirane (35.3 mg, 0.40 mmol) was then added, and the mixture was stirred at 50 °C for 1 h under microwave irradiation and concentrated. The residue was purified using column chromatography on NH silica gel and eluted with MeOH/$CHCl_3$ to obtain **9** as a pale yellow amorphous substance (30 mg, 82%). ^1H NMR (400 MHz, METHANOL-d_4) δ 7.72 (d, $J = 8.2$ Hz, 2H), 7.42 (d, $J = 8.2$ Hz, 2H), 7.15 (s, 1H), 6.92 (s, 1H), 6.70 (s, 1H), 5.56–5.41 (m, 2H), 5.04 (q, $J = 6.6$ Hz, 1H), 3.88–3.70 (m, 1H), 3.47–3.24 (m, 5H), 3.20–3.08 (m, 2H), 2.57–2.38 (m, 4H), 1.95–1.86 (m, 1H), 1.86–1.76 (m, 2H), 1.59 (d, $J = 6.6$ Hz, 3H). ^{13}C NMR (125 MHz, DMSO-d_6) δ 168.8, 161.7, 149.7, 132.0, 126.5, 125.6, 125.5, 125.3, 120.9, 100.0, 94.8, 76.5, 75.3, 67.9, 61.4, 58.3, 57.3, 54.3, 54.1, 40.7, 26.1, 25.9, 21.8, 7.8. LCMS (ESI) *m/z* 463 $[M+H]^+$. Rt 0.565 min (Analytical condition A). HRMS (ESI/APCI dual) *m/z* calcd for $C_{26}H_{30}N_4O_4$ $[M+H]^+$ 463.2340, found 463.2345.

*5.1.8. (1S)-1-{1-[(3-{4-[(1-Aminocyclopropyl)ethynyl]phenyl}-1,2-oxazol-5-yl)methyl]-1H-imidazol-2-yl}ethan-1-ol (**10**)*

A mixture of 3-(4-iodophenyl)-5-[(2-{(1*S*)-1-[(oxan-2-yl)oxy]ethyl}-1*H*-imidazol-1-yl)methyl]-1,2-oxazole **40** (70 mg, 0.15 mmol), CuI (1.4 mg, 0.0073 mmol), $Pd(PPh_3)_4$ (17 mg, 0.015 mmol), Et_3N (0.20 mL, 1.5 mmol), and DMF (0.29 mL) was heated at 65 °C for 5 min, and a solution of *N*-(1-ethynylcyclopropyl)-2,2,2-trifluoroacetamide **28** (34 mg, 0.19 mmol) in DMF (0.38 mL) was then added in a dropwise manner. After stirring for 0.5 h, the mixture was diluted with EtOAc and filtered through a short pad of NH silica gel. The filtrate was concentrated, and the residue was purified using column chromatography on NH silica gel and eluted with EtOAc/*n*-hexane to obtain 2,2,2-trifluoro-*N*-{1-[(4-{5-[(2-{(1*S*)-1-[(oxan-2-yl)oxy]ethyl}-1*H*-imidazol-1-yl)methyl]-1,2-oxazol-3-yl}phenyl)ethynyl]cyclopropyl}acetamide **41** as a crude product, which was dissolved in MeOH (1.5 mL); then, 2 mol/L HCl in MeOH (1.2 mL, 2.4 mmol) was added to the solution at 0 °C. After stirring at the same temperature for 0.5 h, the mixture was stirred at room temperature for 1 h and concentrated to obtain 2,2,2-trifluoro-*N*-[1-({4-[5-({2-[(1*S*)-1-hydroxyethyl]-1*H*-imidazol-1-yl}methyl)-1,2-oxazol-3-yl]phenyl}ethynyl)cyclopropyl]acetamide hydrochloride as a crude product, which was used in the next step without further purification. The crude product was dissolved in MeOH (1.5 mL) followed by the addition of 1 mol/L NaOH solution (1.5 mL, 1.5 mmol) at room temperature. After stirring for 16 h, the mixture was concentrated; the residue was then partitioned between 10% MeOH in $CHCl_3$ and 2 mol/L aqueous Na_2CO_3 solution. The aqueous layer was extracted with 10% MeOH in $CHCl_3$, and the combined organic extracts were dried over $MgSO_4$ and concentrated. The residue was then purified using preparative TLC on silica gel and eluted with $CHCl_3$/MeOH/NH_4OH to obtain **10** as a colorless amorphous substance (41 mg, 81% over three steps). ^{1}H NMR (400 MHz, METHANOL-d_4) δ 7.76 (d, J = 8.7 Hz, 2H), 7.45 (d, J = 8.7 Hz, 2H), 7.20 (s, 1H), 6.94 (s, 1H), 6.73 (s, 1H), 5.61 (dd, J = 14.9, 14.9 Hz, 2H), 5.03 (q, J = 6.4 Hz, 1H), 1.59 (d, J = 6.4 Hz, 3H), 1.08–0.93 (m, 4H). ^{13}C NMR (125 MHz, DMSO-d_6) δ 169.3, 161.4, 149.6, 131.7, 127.3, 126.7, 126.5, 125.0, 121.1, 101.1, 98.3, 77.1, 61.5, 40.8, 24.5, 21.8, 18.0. LCMS (ESI) *m/z* 349 $[M+H]^+$. Rt 0.393 min (Analytical condition A). HRMS (ESI/APCI dual) *m/z* calcd for $C_{20}H_{20}N_4O_2$ $[M+H]^+$ 349.1659, found 349.1667.

*5.1.9. (1S)-1-{1-[(3-{4-[(3-Aminobicyclo[1.1.1]pentan-1-yl)ethynyl]phenyl}-1,2-oxazol-5-yl)methyl]-1H-imidazol-2-yl}ethan-1-ol (**11**)*

A mixture of 3-(4-iodophenyl)-5-[(2-{(1*S*)-1-[(oxan-2-yl)oxy]ethyl}-1*H*-imidazol-1-yl)methyl]-1,2-oxazole **40** (70 mg, 0.15 mmol), CuI (1.4 mg, 0.0073 mmol), $Pd(PPh_3)_4$ (17 mg, 0.015 mmol), Et_3N (0.20 mL, 1.5 mmol), and DMF (0.29 mL) was heated at 65 °C for 5 min, and then a solution of *tert*-butyl (3-ethynylbicyclo[1.1.1]pentan-1-yl)carbamate **29** (39 mg, 0.19 mmol) in DMF (0.38 mL) was added in a dropwise manner. After stirring for 1 h, the mixture was diluted with EtOAc and filtered through a short pad of NH silica gel. The filtrate was concentrated, and the residue was purified using column chromatography on NH silica gel and eluted with EtOAc/*n*-hexane to obtain *tert*-butyl {3-[(4-{5-[(2-{(1*S*)-1-[(oxan-2-yl)oxy]ethyl}-1*H*-imidazol-1-yl)methyl]-1,2-oxazol-3-yl}phenyl)ethynyl]bicyclo[1.1.1]pentan-1-yl}carbamate **42** as a crude product. This product was then dissolved in $CHCl_3$ (0.42 mL), and TFA (0.34 mL) was added to the solution at 0 °C. After stirring at the same temperature for 1 h, the mixture was stirred at room temperature for another 1 h. The mixture was concentrated, and the residue was dissolved in 10% MeOH in $CHCl_3$ (3 mL) and basified with 2 mol/L Na_2CO_3 (3 mL). The phases were separated, and the aqueous layer was extracted with 10% MeOH in $CHCl_3$. The combined organic layer was dried over $MgSO_4$ and concentrated. The residue was purified using preparative TLC on silica gel and eluted with $CHCl_3$/MeOH/NH_4OH to obtain **11** as a colorless amorphous substance (48 mg, 88% over two steps). ^{1}H NMR (400 MHz, METHANOL-d_4) δ 7.75 (d, J = 8.3 Hz, 2H), 7.45 (d, J = 8.3 Hz, 2H), 7.20 (s, 1H), 6.94 (s, 1H), 6.73 (s, 1H), 5.61 (dd, J = 15.7, 15.7 Hz, 2H), 5.03 (q, J = 6.5 Hz, 1H), 2.15 (s, 6H), 1.59 (d, J = 6.5 Hz, 3H). ^{13}C NMR (125 MHz, DMSO-d_6) δ 169.3, 161.4, 149.6, 132.0, 127.8, 126.8, 126.5, 124.4, 121.1, 101.1, 90.4, 80.2, 61.5, 57.4, 50.8, 40.7, 23.8, 21.8. LCMS (ESI) *m/z* 375 $[M+H]^+$. Rt 0.426 min (Analytical condition A). HRMS (ESI/APCI dual) *m/z* calcd for $C_{22}H_{22}N_4O_2$ $[M+H]^+$ 375.1816, found 375.1798.

*5.1.10. 1-[(1R,5S,6s)-6-({4-[5-({2-[(1S)-1-Hydroxyethyl]-1H-imidazol-1-yl}methyl)-1,2-oxazol-3-yl]phenyl}ethynyl)-3-azabicyclo[3.1.0]hexan-3-yl]-3-methoxypropan-2-ol (**12**)*

2-(Methoxymethyl)oxirane (34 mg, 0.39 mmol) was added to a suspension of (1*S*)-1-(1-{[3-(4-{[(1*R*,5*S*,6*s*)-3-azabicyclo[3.1.0]hexan-6-yl]ethynyl}phenyl)-1,2-oxazol-5-yl]methyl}-1*H*-imidazol-2-yl)ethan-1-ol **44** (29 mg, 0.077 mmol) in EtOH (1 mL). After stirring at room temperature overnight, MeOH (1 mL) and 2-(methoxymethyl)oxirane (15 mg, 0.17 mmol) were added to the mixture, which was stirred at 60 °C for 1 h and concentrated. The residue was purified using column chromatography on NH silica gel and eluted with MeOH/$CHCl_3$ to obtain **12** as a light yellow amorphous substance (27 mg, 75%). ^{1}H NMR (400 MHz, METHANOL-d_4) δ 7.73 (d, J = 8.1 Hz, 2H), 7.41 (d, J = 8.1 Hz, 2H), 7.19 (s, 1H), 6.94 (s, 1H), 6.72 (s, 1H), 5.68–5.53 (m, 2H), 5.03 (q, J = 6.6 Hz, 1H), 3.83–3.74 (m, 1H), 3.42–3.36 (m, 2H), 3.35 (s, 3H), 3.15 (br dd, J = 9.0, 5.2 Hz, 2H), 2.54–2.38 (m, 4H), 1.92–1.87 (m, 1H), 1.83–1.78 (m, 2H), 1.59 (d, J = 6.6 Hz, 3H). ^{13}C NMR (125 MHz, DMSO-d_6) δ 169.2, 161.4, 149.6, 131.9, 127.3, 126.7, 126.5, 125.1, 121.0, 101.1, 94.2, 76.5, 75.3, 67.9, 61.5, 58.3, 57.3, 54.2, 54.1, 40.7, 26.1, 25.8, 21.8, 7.7. LCMS (ESI) *m/z* 463 $[M+H]^+$. Rt 0.560 min (Analytical condition A). HRMS (ESI/APCI dual) *m/z* calcd for $C_{26}H_{30}N_4O_4$ $[M+H]^+$ 463.2340, found 463.2326.

*5.1.11. (1S)-1-{1-[(1R)-2-Amino-1-(5-{4-[(1-aminocyclopropyl)ethynyl]phenyl}-1,2-oxazol-3-yl)ethyl]-1H-imidazol-2-yl}ethan-1-ol (**13**)*

Two mol/L Na_2CO_3 (0.26 mL, 0.53 mmol) was added to a mixture of *tert*-butyl [(2*R*)-2-(5-iodo-1,2-oxazol-3-yl)-2-(2-{(1*S*)-1-[(oxan-2-yl)oxy]ethyl}-1*H*-imidazol-1-yl)ethyl]carbamate **45** (70 mg, 0.13 mmol), *tert*-butyl (1-{[4-(4,4,5,5-tetramethyl-1,3,2-dioxaborolan-2-yl)phenyl]ethynyl}cyclopropyl)carbamate **47** (76 mg, 0.20 mmol), and Pd-PEPPSI-IPent catalyst (10 mg, 0.013 mmol) in toluene (0.53 mL) and EtOH (0.53 mL). After stirring at 100 °C for 2 h, EtOAc and saturated aqueous $NaHCO_3$ were added to the mixture, which was extracted with EtOAc. The separated organic extract was dried over $MgSO_4$ and concentrated. The residue was purified using column chromatography on silica gel and eluted with MeOH/$CHCl_3$ to obtain *tert*-butyl [(2*R*)-2-{5-[4-({1-[(*tert*-butoxycarbonyl)amino]cyclopropyl}ethynyl)phenyl]-1,2-oxazol-3-yl}-2-(2-{(1*S*)-1-[(oxan-2-yl)oxy]ethyl}-1*H*-imidazol-1-yl)ethyl]carbamate **51** as a crude product [LCMS (ESI) *m/z* 662 $[M+H]^+$. Rt 0.932 min (Analytical condition B)], which was taken up in $CHCl_3$ (2.2 mL). TFA (0.42 mL, 5.4 mmol) was added, and the mixture was stirred at room temperature for 2 h, then basified with saturated aqueous K_2CO_3 at 0 °C and extracted with 10% MeOH in $CHCl_3$ ten times. The combined organic extracts were passed through a phase separator and concentrated. The residue was purified using column chromatography on silica gel and eluted with $CHCl_3$/MeOH/NH_4OH, then purified again using column chromatography on NH silica gel and eluted with MeOH/$CHCl_3$ to obtain **13** as a pale yellow amorphous substance (10 mg, 20% over two steps). ^{1}H NMR (600 MHz, METHANOL-d_4) δ 7.76 (d, J = 8.3 Hz, 2H), 7.47 (d, J = 8.3 Hz, 2H), 7.24 (d, J = 1.2 Hz, 1H), 6.97 (d, J = 1.2 Hz, 1H), 6.78 (s, 1H), 5.93–5.88 (m, 1H), 5.09 (q, J = 6.6 Hz, 1H), 3.52 (dd, J = 13.6, 6.2 Hz, 1H), 3.39 (dd, J = 13.6, 8.3 Hz, 1H), 1.66 (d, J = 6.6 Hz, 3H), 1.06–1.02 (m, 2H), 1.00–0.96 (m, 2H). ^{13}C NMR (125 MHz, DMSO-d_6) δ 168.7, 163.5, 150.1, 131.8, 126.9, 125.6, 125.6, 125.2, 117.6, 100.0, 98.9, 77.1, 60.8, 54.1, 44.8, 24.5, 21.5, 18.1. LCMS (ESI) *m/z* 189 $[M + 2H]^{2+}$. Rt 0.201 min (Analytical condition A). HRMS (ESI/APCI dual) *m/z* calcd for $C_{21}H_{23}N_5O_2$ $[M+H]^+$ 378.1925, found 378.1910.

*5.1.12. (1S)-1-{1-[(1R)-2-Amino-1-(5-{4-[(3-aminobicyclo[1.1.1]pentan-1-yl)ethynyl]phenyl}-1,2-oxazol-3-yl)ethyl]-1H-imidazol-2-yl}ethan-1-ol **(14)***

A mixture of intermediate *tert*-butyl [(2*R*)-2-(5-iodo-1,2-oxazol-3-yl)-2-(2-{(1*S*)-1-[(oxan-2-yl)oxy]ethyl}-1*H*-imidazol-1-yl)ethyl]carbamate **45** (170 mg, 0.32 mmol), *tert*-butyl (3-{[4-(4,4,5,5-tetramethyl-1,3,2-dioxaborolan-2-yl)phenyl]ethynyl}bicyclo[1.1.1]pentan-1-yl) carbamate **48** (170 mg, 0.42 mmol), Pd-PEPPSI-IPent catalyst (25 mg, 0.032 mmol), and 2 mol/L Na_2CO_3 (0.64 mL, 1.3 mmol) in toluene (1.6 mL) and EtOH (1.6 mL) was stirred at 80 °C for 1 h. The mixture was poured into 2 mol/L Na_2CO_3 and extracted with EtOAc three times. The combined organic extracts were washed with brine, dried over $MgSO_4$ and concentrated. The residue was purified using column chromatography on NH silica gel and eluted with EtOAc/*n*-hexane to obtain *tert*-butyl [(2*R*)-2-{5-[4-({3-[(*tert*-butoxycarbonyl)amino]bicyclo[1.1.1]pentan-1-yl}ethynyl)phenyl]-1,2-oxazol-3-yl}-2-(2-{(1*S*)-1-[(oxan-2-yl)oxy]ethyl}-1*H*-imidazol-1-yl)ethyl]carbamate **52** as a crude product, which was used in the next step without further purification.

TFA (0.81 mL, 11 mmol) was added to a solution of **52** in $CHCl_3$ (1.4 mL) at room temperature. After stirring for 45 min, MeOH (1.5 mL) was added, and the resulting mixture was stirred at that temperature for another 0.5 h and concentrated. The residue was partitioned between 2 mol/L Na_2CO_3 and 10% MeOH in $CHCl_3$. The aqueous layer was extracted four times with 10% MeOH in $CHCl_3$. The combined organic extracts were dried over $MgSO_4$ and concentrated. The residue was purified using preparative TLC on silica gel and eluted with $CHCl_3$/MeOH/NH_4OH to obtain **14** as a pale yellow amorphous substance (40 mg, 31% over two steps). ^{1}H NMR (600 MHz, METHANOL-d_4) δ 7.75 (d, J = 8.3 Hz, 2H), 7.46 (d, J = 8.3 Hz, 2H), 7.24 (s, 1H), 6.97 (s, 1H), 6.79 (s, 1H), 5.90 (dd, J = 8.1, 6.2 Hz, 1H), 5.09 (q, J = 6.3 Hz, 1H), 3.52 (dd, J = 13.6, 6.2 Hz, 1H), 3.39 (dd, J = 13.6, 8.1 Hz, 1H), 2.12 (s, 6H), 1.66 (d, J = 6.3 Hz, 3H). ^{13}C NMR (125 MHz, DMSO-d_6) δ 168.6, 163.5, 150.1, 132.1, 126.9, 125.9, 125.7, 124.6, 117.6, 100.1, 91.3, 80.1, 60.8, 57.6, 54.1, 51.6, 44.8, 23.6, 21.5. LCMS (ESI) m/z 404 $[M+H]^+$. Rt 0.221 min (Analytical condition A). HRMS (ESI/APCI dual) m/z calcd for $C_{23}H_{25}N_5O_2$ $[M+H]^+$ 404.2081, found 404.2076.

*5.1.13. (1R,3r)-3-[(4-{3-[(1R)-2-Amino-1-{2-[(1S)-1-hydroxyethyl]-1H-imidazol-1-yl}ethyl]-1,2-oxazol-5-yl}phenyl)ethynyl]cyclobutan-1-ol **(15)***

Four mol/L HCl in 1,4-dioxane (10 mL) was added to a solution of *tert*-butyl [(2*R*)-2-[5-(4-{[(1*r*,3*R*)-3-{[*tert*-butyl(dimethyl)silyl]oxy}cyclobutyl]ethynyl}phenyl)-1,2-oxazol-3-yl]-2-{2-[(1*S*)-1-{[*tert*-butyl(dimethyl)silyl]oxy}ethyl]-1*H*-imidazol-1-yl}ethyl]carbamate **53** (0.535 mg, 0.74 mmol) in MeOH (1 mL). The mixture was stirred at room temperature for 5 h and concentrated. The residue was basified with 20% aqueous K_2CO_3 and extracted with a combined solvent of $CHCl_3$ and MeOH. The separated organic extract was passed through a phase separator and concentrated. The residue was purified using column chromatography on NH silica gel and eluted with MeOH/$CHCl_3$ to obtain **15** as a colorless amorphous substance (274 mg, 94%). ^{1}H NMR (400 MHz, CHLOROFORM-*d*) δ 7.66 (d, J = 8.1 Hz, 2H), 7.47 (d, J = 8.1 Hz, 2H), 7.09 (s, 1H), 6.96 (s, 1H), 6.30 (s, 1H), 5.65 (br dd, J = 9.4, 3.8 Hz, 1H), 5.05 (q, J = 6.4 Hz, 1H), 4.72–4.60 (m, 1H), 3.63 (br dd, J = 13.4, 3.8 Hz, 1H), 3.52–3.39 (m, 1H), 3.31–3.18 (m, 1H), 2.58–2.46 (m, 2H), 2.40–2.24 (m, 2H), 1.77 (d, J = 6.4 Hz, 3H). ^{13}C NMR (125 MHz, DMSO-d_6) δ 168.7, 163.5, 150.1, 132.0, 126.9, 125.6, 125.2, 117.6, 100.0, 97.4, 80.0, 64.4, 60.8, 54.1, 44.9, 21.5, 17.4. LCMS (ESI) m/z 393 $[M+H]^+$. Rt 0.710 min (Analytical condition A). HRMS (ESI/APCI dual) m/z calcd for $C_{22}H_{24}N_4O_3$ $[M+H]^+$ 393.1921, found 393.1902.

*5.1.14. (1R,5S,6s)-6-({4-[3-({2-[(1S)-1-Hydroxyethyl]-1H-imidazol-1-yl}methyl)-1,2-oxazol-5-yl]phenyl}ethynyl)-3-azabicyclo[3.1.0]hexane-3-carbaldehyde **(16)***

N-Formylsaccharin (12 mg, 0.057 mmol) was added to a solution of (1*S*)-1-(1-{[5-(4-{[(1*R*,5*S*,6*s*)-3-azabicyclo[3.1.0]hexan-6-yl]ethynyl}phenyl)-1,2-oxazol-3-yl]methyl}-1*H*-imidazol-2-yl)ethan-1-ol **37** (20 mg, 0.053 mmol) in THF (1 mL) and DMF (0.5 mL). After stirring at room temperature for 1 h, the mixture was diluted with $CHCl_3$ and saturated aqueous $NaHCO_3$, then extracted with a combined solvent of $CHCl_3$ and MeOH. The organic extract was concentrated, and the residue was purified using column chromatography on NH silica gel and eluted with MeOH/EtOAc to obtain **16** as a colorless solid (15 mg, 70%). ^{1}H NMR (400 MHz, METHANOL-d_4) δ 8.10 (s, 1H), 7.73 (d, J = 8.2 Hz, 2H), 7.45 (d, J = 8.2 Hz, 2H), 7.15 (s, 1H), 6.92 (s, 1H), 6.71 (s, 1H), 5.56–5.41 (m, 2H), 5.04 (br q, J = 6.6 Hz, 1H), 3.95–3.79 (m, 2H), 3.72–3.64 (m, 1H), 3.39–3.23 (m, 1H), 2.09–1.97 (m, 2H), 1.59 (d, J = 6.6 Hz, 3H), 1.39–1.33 (m, 1H). ^{13}C NMR (125 MHz, DMSO-d_6) δ 168.7, 161.8, 161.7, 149.7, 132.1, 126.5, 125.7, 124.9, 120.9, 100.1, 92.9, 77.3, 61.4, 47.2, 44.4, 40.6, 24.8, 24.7, 21.8, 9.7. LCMS (ESI) m/z 403 $[M+H]^+$. Rt 0.838 min (Analytical condition A). HRMS (ESI/APCI dual) m/z calcd for $C_{23}H_{22}N_4O_3$ $[M+H]^+$ 403.1765, found 403.1747.

*5.1.15. (1R,5S,6s)-6-[(4-{3-[(1R)-2-Amino-1-{2-[(1S)-1-hydroxyethyl]-1H-imidazol-1-yl}ethyl]-1,2-oxazol-5-yl}phenyl)ethynyl]-3-azabicyclo[3.1.0]hexane-3-carbaldehyde **(17)***

In step 1, *N*-formylsaccharin (189 mg, 0.90 mmol) was added to a solution of *tert*-butyl [(2*R*)-2-[5-(4-{[(1*R*,5*S*,6*s*)-3-azabicyclo[3.1.0]hexan-6-yl]ethynyl}phenyl)-1,2-oxazol-3-yl]-2-{2-[(1*S*)-1-hydroxyethyl]-1*H*-imidazol-1-yl}ethyl]carbamate **55** (410 mg, 0.81 mmol) in THF (8.1 mL). After stirring at room temperature for 40 min, saturated aqueous $NaHCO_3$ was added to the mixture at 0 °C and extracted with $CHCl_3$. The organic extract was passed through a phase separator and concentrated. The residue was purified using column chromatography on NH silica gel and eluted with MeOH/EtOAc to obtain *tert*-butyl [(2*R*)-2-[5-(4-{[(1*R*,5*S*,6*s*)-3-formyl-3-azabicyclo[3.1.0]hexan-6-yl]ethynyl}phenyl)-1,2-oxazol-3-yl]-2-{2-[(1*S*)-1-hydroxyethyl]-1*H*-imidazol-1-yl}ethyl]carbamate as a colorless solid (386 mg, 89%). LCMS (ESI) m/z 532 $[M+H]^+$. Rt 0.659 min (Analytical condition B).

In step 2, 4 mol/L HCl in 1,4-dioxane (9.0 mL, 36 mmol) was added to a solution of the above-described solid (384 mg, 0.72 mmol) in MeOH (7.2 mL) at 0 °C. The mixture was stirred at room temperature for 1 h and concentrated. The residue was basified with 20% aqueous K_2CO_3 and a combined solvent of $CHCl_3$ and MeOH. The organic extract was passed through a phase separator and concentrated. The residue was purified using column chromatography on silica gel and eluted with MeOH containing 28% aqueous ammonia/$CHCl_3$ to obtain **17** as a colorless solid (264 mg, 85%). ^{1}H NMR (400 MHz, METHANOL-d_4) δ 8.10 (s, 1H), 7.74 (d, J = 7.8 Hz, 2H), 7.45 (d, J = 7.8 Hz, 2H), 7.24 (s, 1H), 6.97 (s, 1H), 6.77 (s, 1H), 5.94–5.85 (m, 1H), 5.14–5.03 (m, 1H), 3.96–3.78 (m, 2H), 3.75–3.61 (m, 1H), 3.59–3.46 (m, 1H), 3.45–3.16 (m, 2H), 2.09–1.96 (m, 2H), 1.66 (d, J = 6.4 Hz, 3H), 1.39–1.33 (m, 1H). ^{13}C NMR (125 MHz, DMSO-d_6) δ 168.6, 163.5, 161.7, 150.1, 132.1, 126.9, 125.7, 125.6, 124.9, 117.6, 100.0, 92.9, 77.3, 60.8, 54.1, 47.2, 44.9, 44.4, 24.8, 24.7, 21.5, 9.6. LCMS (ESI) m/z 432 $[M+H]^+$. Rt 0.652 min (Analytical condition A). HRMS (ESI/APCI dual) m/z calcd for $C_{24}H_{25}N_5O_3$ $[M+H]^+$ 432.2030, found 432.2025.

*5.1.16. (S)-1-((1R,5S,6R)-6-((4-(3-((R)-2-Amino-1-(2-((S)-1-hydroxyethyl)-1H-imidazol-1-yl)ethyl)isoxazol-5-yl)phenyl)ethynyl)-3-azabicyclo[3.1.0]hexan-3-yl)propan-2-ol **(18)***

(2*S*)-2-Methyloxirane (0.042 mL, 0.60 mmol) was added to a solution of *tert*-butyl [(2*R*)-2-[5-(4-{[(1*R*,5*S*,6*s*)-3-azabicyclo[3.1.0]hexan-6-yl]ethynyl}phenyl)-1,2-oxazol-3-yl]-2-{2-[(1*S*)-1-hydroxyethyl]-1*H*-imidazol-1-yl}ethyl]carbamate **55** (20 mg, 0.040 mmol) in MeOH (1 mL). The mixture was stirred at 50 °C for 1.5 h under microwave irradiation. Additional (2*S*)-2-methyloxirane (0.042 mL, 0.60 mmol) was added, and the mixture was stirred at 50 °C for 1 h under microwave irradiation and concentrated. The residue was purified using column chromatography on NH silica gel and eluted with MeOH/EtOAc to obtain *tert*-butyl [(2*R*)-2-{2-[(1*S*)-1-hydroxyethyl]-1*H*-imidazol-1-yl}-2-

{5-[4-({(1*R*,5*S*,6*R*)-3-[(2*S*)-2-hydroxypropyl]-3-azabicyclo[3.1.0]hexan-6-yl}ethynyl)phenyl]-1,2-oxazol-3-yl}ethyl]carbamate as a crude product, which was dissolved in MeOH (5 mL). Then, 4 mol/L HCl in 1,4-dioxane (1.0 mL, 4.0 mmol) was added to the solution. The mixture was stirred at room temperature for 1 h and concentrated. The residue was basified with 20% aqueous K_2CO_3 and extracted with a combined solvent of $CHCl_3$ and MeOH. The organic extract was passed through a phase separator and concentrated. The residue was purified using column chromatography on NH silica gel and eluted with MeOH/$CHCl_3$ to obtain **18** as a pale yellow solid (19 mg, quant over two steps). ^{1}H NMR (400 MHz, METHANOL-d_4) δ 7.73 (d, J = 8.0 Hz, 2H), 7.42 (d, J = 8.0 Hz, 2H), 7.24 (s, 1H), 6.97 (s, 1H), 6.75 (s, 1H), 5.90 (t, J = 6.9 Hz, 1H), 5.14–5.03 (m, 1H), 3.88–3.05 (m, 5H), 2.51–2.26 (m, 4H), 1.97–1.90 (m, 1H), 1.85–1.77 (m, 2H), 1.66 (d, J = 6.2 Hz, 3H), 1.11 (d, J = 5.6 Hz, 3H). ^{13}C NMR (125 MHz, DMSO-d_6) δ 168.7, 163.5, 150.1, 132.0, 126.9, 125.6, 125.5, 125.3, 117.6, 99.9, 94.9, 76.4, 64.5, 61.9, 60.8, 54.1, 54.1, 54.0, 44.9, 26.1, 25.9, 21.5, 21.4, 7.7. LCMS (ESI) m/z 462 $[M+H]^+$. Rt 0.211 min (Analytical condition A). HRMS (ESI/APCI dual) m/z calcd for $C_{26}H_{31}N_5O_3$ $[M+H]^+$ 462.2500, found 462.2488.

5.1.17. 4-[(1R,5S,6s)-6-({4-[3-({2-[(1S)-1-Hydroxyethyl]-1H-imidazol-1-yl}methyl)-1,2-oxazol-5-yl]phenyl}ethynyl)-3-azabicyclo[3.1.0]hexan-3-yl]butanoic acid (19)

In step 1, K_2CO_3 (332 mg, 2.40 mmol) and NaI (120 mg, 0.80 mmol) were added to a mixture of (1*S*)-1-(1-{[5-(4-{[(1*R*,5*S*,6*s*)-3-azabicyclo[3.1.0]hexan-6-yl]ethynyl}phenyl)-1,2-oxazol-3-yl]methyl}-1*H*-imidazol-2-yl)ethan-1-ol **37** (300 mg, 0.80 mmol) and ethyl 4-bromobutanoate (172 mg, 0.88 mmol) in DMF (7.5 mL). After stirring at 80 °C for 80 min, 20% aqueous K_2CO_3 was added to the mixture, which was extracted with EtOAc. The separated organic extract was washed twice with 20% aqueous K_2CO_3 and concentrated. The residue was purified using column chromatography on NH silica gel and eluted with EtOAc/*n*-hexane and MeOH/$CHCl_3$ to obtain ethyl 4-[(1*R*,5*S*,6*s*)-6-({4-[3-({2-[(1*S*)-1-hydroxyethyl]-1*H*-imidazol-1-yl}methyl)-1,2-oxazol-5-yl]phenyl}ethynyl)-3-azabicyclo[3.1.0]hexan-3-yl]butanoate as a pale yellow amorphous substance (293 mg, 75%). LCMS (ESI) m/z 245 $[M+2H]^{2+}$. Rt 0.834 min (Analytical condition A).

In step 2, 2 mol/L NaOH solution (3.0 mL, 6.0 mmol) was added to a solution of the above-described substance (291 mg, 0.60 mmol) in MeOH (3 mL) and THF (3 mL). After stirring at room temperature for 2 h, the mixture was neutralized with 1 mol/L hydrochloric acid at 0 °C and concentrated. The residue was purified using Diaion HP-20 to obtain **19** as a pale yellow amorphous substance (212 mg, 77%). ^{1}H NMR (400 MHz, METHANOL-d_4) δ 7.73 (d, J = 8.2 Hz, 2H), 7.44 (d, J = 8.2 Hz, 2H), 7.15 (s, 1H), 6.93 (s, 1H), 6.71 (s, 1H), 5.56–5.41 (m, 2H), 5.04 (q, J = 6.6 Hz, 1H), 3.62 (d, J = 11.0 Hz, 2H), 3.09 (br d, J = 10.6 Hz, 2H), 3.03 (br t, J = 6.0 Hz, 2H), 2.47–2.39 (m, 2H), 2.15–2.10 (m, 2H), 1.88–1.79 (m, 3H), 1.59 (d, J = 6.6 Hz, 3H). ^{13}C NMR (125 MHz, DMSO-d_6) δ 174.4, 168.8, 161.8, 149.7, 132.0, 126.5, 125.7, 125.5, 125.3, 120.9, 100.1, 94.7, 76.5, 61.4, 53.5, 53.3, 40.7, 31.7, 26.0, 23.4, 21.8, 7.9. LCMS (ESI) m/z 461 $[M+H]^+$. Rt 0.641 min (Analytical condition A). HRMS (ESI/APCI dual) m/z calcd for $C_{26}H_{28}N_4O_4$ $[M+H]^+$ 461.2183, found 461.2169.

5.1.18. 4-{(1R,5S,6s)-6-[(4-{3-[(1R)-2-Amino-1-{2-[(1S)-1-hydroxyethyl]-1H-imidazol-1-yl}ethyl]-1,2-oxazol-5-yl}phenyl)ethynyl]-3-azabicyclo[3.1.0]hexan-3-yl}butanoic acid (20)

In step 1, 4 mol/L HCl in 1,4-dioxane (2.0 mL, 8.0 mmol) was added to a solution of ethyl 4-{(1*R*,5*S*,6*s*)-6-[(4-{3-[(1*R*)-2-[(*tert*-butoxycarbonyl)amino]-1-{2-[(1*S*)-1-hydroxyethyl]-1*H*-imidazol-1-yl}ethyl]-1,2-oxazol-5-yl}phenyl)ethynyl]-3-azabicyclo[3.1.0]hexan-3-yl}butanoate **57** (73 mg, 0.12 mmol) in MeOH (0.1 mL). The mixture was stirred at room temperature for 1 h and concentrated to obtain ethyl 4-{(1*R*,5*S*,6*s*)-6-[(4-{3-[(1*R*)-2-amino-1-{2-[(1*S*)-1-hydroxyethyl]-1*H*-imidazol-1-yl}ethyl]-1,2-oxazol-5-yl}phenyl)ethynyl]-3-azabicyclo[3.1.0]hexan-3-yl}butanoate hydrogen chloride as a crude product, which was used in the next step without further purification. LCMS (ESI) m/z 518 $[M+H]^+$. Rt 0.592 min (Analytical condition A).

In step 2, the above-described product was taken up in THF (2 mL). To this suspension, 1 mol/L aqueous NaOH (2 mL, 4 mmol) was added. The mixture was stirred at room temperature for 2 h, neutralized with 1 mol/L hydrochloric acid, and washed with EtOAc. The separated aqueous layer was purified using Diaion HP-20 to obtain **20** as a pale yellow solid (19 mg, 34% over two steps). ^{1}H NMR (400 MHz, METHANOL-d_4) δ 7.74 (d, J = 8.2 Hz, 2H), 7.44 (d, J = 8.2 Hz, 2H), 7.24 (s, 1H), 6.98 (s, 1H), 6.77 (s, 1H), 5.92 (br t, J = 7.2 Hz, 1H), 5.09 (q, J = 6.5 Hz, 1H), 3.58–3.34 (m, 4H), 2.91–2.80 (m, 4H), 2.34 (br t, J = 6.5 Hz, 2H), 2.06–2.00 (m, 2H), 1.88–1.75 (m, 3H), 1.66 (d, J = 6.5 Hz, 3H). ^{13}C NMR (125 MHz, DMSO-d_6) δ 174.8, 168.7, 163.5, 150.1, 132.0, 126.9, 125.6, 125.5, 125.3, 117.6, 99.9, 94.8, 76.4, 60.8, 54.1, 53.6, 53.5, 44.9, 32.7, 26.0, 24.0, 21.5, 7.9. LCMS (ESI) m/z 490 $[M+H]^+$. Rt 0.514 min (Analytical condition A). HRMS (ESI/APCI dual) m/z calcd for $C_{27}H_{31}N_5O_4$ $[M+H]^+$ 490.2449, found 490.2442.

5.2. Evaluation of the inhibitory activity on E. coli LpxC

The IC_{50} of *E. coli* LpxC was determined using the synthetic lipid substrate UDP-3-*O*-(*R*-3-hydroxymyristoyl)-*N*-acetylglucosamine, as described previously with slight modifications.[28,29] *E. coli* LpxC purified from *E. coli* cells was used for the assay. An LpxC enzyme assay was performed with reaction mixtures containing 40 mM MES (pH6.5), 0.02v/v% Brij35, 80 μM dithiothreitol, 25 nM $ZnCl_2$, 3.1 nM *E. coli* LpxC and 20 μM UDP-3-*O*-(*R*-3-hydroxymyristoyl)-*N*-acetylglucosamine. The reaction mixtures were incubated for 120 min at room temperature. For the fluorescamine assay, the reaction was terminated by the addition of 0.2 M sodium phosphate buffer and 1.0 mg/mL fluorescamine in a 1:1 vol mixture of *N*,*N*-dimethylformamide and acetonitrile. Fluorescence (390 nm excitation/495 nm emission) was detected using an EnSpire instrument (PerkinElmer Japan Co., Ltd., Tokyo, Japan). For the LCMS assay, the reaction terminated by the addition of acetonitrile containing 25 μM UDP-GlcNAc was used as an internal standard. The mixture was centrifuged, and the supernatant was injected into a liquid chromatography-tandem mass spectrometry (LC-MS/MS) instrument. The samples were separated using an Inertsil Amide column (3.0 μm, 50 mm × 2.1 mm I.D.; GLScience, Japan) using the Shimadzu HPLC system. The mobile phase was 8 mM ammonium acetate containing 72% acetonitrile, and the flow rate was 0.2 mL/min. MS/MS detection of each component was performed using a TSQ Quantum system (Thermo Fisher Scientific, USA) or a QTRAP-5500 system (SCIEX, USA) with an electrospray interface in negative ion detection mode. The inhibition values were calculated from the product signals of the control DMSO samples containing no compound (0% inhibition) and samples containing no substrate (100% inhibition).

5.3. Evaluation of antibacterial activity

The MIC was determined using the Clinical and Laboratory Standards Institute (CLSI) broth micro-dilution method.[30]

5.4. In vivo models

All *in vivo* experimental protocols used in this study were approved by the Taisho Pharmaceutical Animal Care Committee and were in accordance with the Guidelines for Proper Conduct of Animal Experiments (Science Council of Japan, 2006). Animals were maintained under controlled temperature (23 ± 3 °C) and humidity (50 ± 20%) conditions and a 12-h light/dark cycle (lights on at 07:00 h).

5.5. Efficacy studies

5.5.1. Murine systemic infection model

Four-week-old male ICR mice (Japan SLC, Inc., Shizuoka, Japan)

were inoculated intraperitoneally with 0.5 mL of bacterial suspension including 3w/v% mucin (Sigma-Aldrich). The challenge doses of *K. pneumoniae* 4102 were 3.8–5.5 × 10^6 CFU/mouse. The test compounds were subcutaneously administered at 1 h after inoculation (n = 6). The survival rates of each group were evaluated for 7 days. The test compounds were dissolved in 10w/v% hydroxypropyl-β-cyclodextrin (HP-β-CD; NIHON SHOKUHIN KAKO CO., LTD., Tokyo, Japan). All the vehicle-treated mice (10w/v% HP-β-CD) died after inoculation.

5.5.2. Murine lung infection model

Five-week-old female ICR mice (Japan SLC, Inc.) were used in this study. Neutropenia was induced with the intraperitoneal administration of 150 and 100 mg/kg of cyclophosphamide (SHIONOGI & CO., LTD., Osaka, Japan) at 4 days and 1 day prior to infection, respectively. Mice were inoculated intranasally with 0.05 mL of bacterial suspension (1.5–1.9 × 10^6 CFU/mouse) of *K. pneumoniae* ATCC BAA-2343 (bla_{KPC+}). The test compounds were subcutaneously administered at 2 h after inoculation (n = 5). Viable cells in the lungs were counted at 2 (control) and 26 h after inoculation. The test compounds were dissolved in 10w/v% HP-β-CD.

5.6. Protein binding assay

The protein binding assay was conducted using a 96-well equilibrium dialysis method. The pooled serum of male ICR mice was obtained from Charles River Laboratories Japan, Inc. Guinea pigs serum was obtained from male Hartley guinea pigs (Japan SLC, Inc.) by venous puncture and were collected without the use of an anticoagulant. Human serum was obtained from healthy male and female volunteers by venous puncture and were collected without the use of an anticoagulant. The compounds were diluted in serum to yield final concentrations of 1 μg/mL (human and mouse) and 500 μg/mL (guinea pig). Serum samples were dialyzed using a dialysis membrane (molecular weight cut-off: 12000–14000 Da) against 50 mM sodium phosphate buffer at 37 °C for 4 h in a 5% CO_2-incubator. The concentration of the test compound on each side of the membrane was determined using LC-MS/MS. The serum protein binding ability was calculated using the following equation:

$$\text{Serum protein binding } (\%) = (C_s - C_b)/C_s \times 100,$$

where C_s and C_b represent the concentration of the test compound in the serum and buffer, respectively.

The unbound fraction in guinea pig serum was calculated using the following equation:

$$\text{Fraction unbound in serum} = 1 - (\text{Serum protein binding})/100.$$

5.7. Cardiovascular study

The maintenance and experimental protocols conformed to the Guide for the Care and Use of Laboratory Animals of Taisho Pharmaceutical Co., Ltd.

Two cardiovascular studies were conducted to assess the effects of the test compounds. Compounds **15** and **19** (**TP0586532**) were assessed in the first study, and compounds **17** and **18** were assessed in the second. Male Hartley guinea pigs were obtained from Japan SLC, Inc. (Shizuoka, Japan). An aqueous solution (concentration, 11w/v%; pH4) of sulfobutyl ether-β-cyclodextrin (SBE-β-CD; Cyclolab Cyclodextrin Research and Development Laboratory Ltd., Budapest, Hungary) was used in the vehicle control group in both studies.

Six- to seven-week-old guinea pigs were anesthetized with pentobarbital (60 mg/kg, double dilution with saline, intraperitoneal administration) and placed in a supine position on a thermal heated plate during surgery. A tube was cannulated into the trachea and connected to a ventilator. The artificial respiration conditions were 15 mL/kg and 60 times/min. A polyethylene tube filled with pentobarbital was cannulated into the femoral vein. The infusion rate for pentobarbital was 8 mg/kg/h. Another polyethylene tube filled with saline was cannulated into the jugular vein and was used for the administration of the vehicle or test compounds. A measurement cannula filled with heparinized saline connected to a pressure transducer was cannulated into the carotid artery to measure blood pressure using a blood pressure amplifier. Electrocardiography was performed using an electrocardiogram amplifier. The anesthetized guinea pigs were intravenously administered infusions of the vehicle or test compounds for 30 min. The QTc was calculated by correcting the QT interval in Bazett's formula. Heart rate, QTc, systolic blood pressure, and diastolic blood pressure were recorded as the change from the baseline value.

Blood was collected at the end of the infusion period and was centrifuged to obtain the plasma for the exposure assessment. The plasma concentration at the end of infusion (C_{30min}) was determined using a LC-MS/MS system (AB SCIEX, Framingham, MA). The unbound plasma concentration at the end of infusion ($C_{30min,\ free}$) was calculated by multiplying the C_{30min} value and the unbound fraction in plasma, which was assumed to be equal to the unbound fraction in serum.

5.8. MTD and repeated dose studies

Exploratory MTD studies were conducted using male ICR mice (Charles River Laboratories Japan, Inc., Kanagawa, Japan) at dose levels of up to 200 mg/kg using a single intravenous injection via the tail vein.

For the repeated dose studies, **TP0586532** was intravenously administered to 6-week-old male and female Sprague Dawley (SD) rats (Charles River Laboratories Japan, Inc., Kanagawa, Japan) for 4 days (bolus, via tail vein) and to 3-year-old female cynomolgus monkeys (Vanny Bio-Research [Cambodia] Corporation Ltd., Cambodia) for 14 days (infusion for 30 min, via saphenous vein) to assess the MTDs using repeated dosing.

5.9. hERG channel assay

An automated patch clamp method (Q-Patch^{HTX}) (Sophion Bioscience, Ballerup, Denmark) was used to evaluate the effects of 8-(methylamino)-2-oxo-1,2-dihydroquinoline derivatives on the hERG potassium channel. Q cell (CHO hERG Duo optimized for the Q-patch) was purchased from Sophion Bioscience, and the experiment was conducted in accordance with their protocol. The IC_{50} values of compounds **15**, **17**, **18**, and **19** (**TP0586532**) and of quinidine (positive control) on whole-cell hERG currents were determined.

5.10. Protein production

P. aeruginosa LpxC(1–299) carrying the C40S mutation was expressed and purified as reported previously.[20]

5.11. Crystallization, data collection and processing

Complexes with inhibitors were crystallized using the sitting drop vapor diffusion method at 293 K. Crystals were flash-frozen and were measured at a temperature of 100 K. Diffraction data for the cocrystals was collected at either the beamline BL45XU of SPring-8 (Japan) or in-house using a MicroMax 007 HF Generator (Rigaku) with a PILATUS 200 K (Rigaku). Data processing was performed using CrysAlisPro (Rigaku). The structure was determined using molecular replacement with MolRep and the structure of the PDB code of 3UHM as the search model. The structure was refined with Refmac5. The data collection and refinement statistics are summarized in the Supplementary Data (Table S1).

Declaration of Competing Interest

The authors declare that they have no known competing financial

interests or personal relationships that could have appeared to influence the work reported in this paper.

Acknowledgments

The authors thank Dr. Takashi Yoshizumi for his contributions to the project, Maho Honda-Yamagishi and Toru Yamaguchi-Sasaki for the preparation of the compounds, Reiko Wada for performing the hERG channel assay, Dr. Atsushi Okada for recording the nuclear magnetic resonance spectra, and Akira Higuchi for recording the high-resolution mass spectra.

Appendix A. Supplementary material

Supplementary data to this article can be found online at https://doi.org/10.1016/j.bmc.2020.115964.

References

1 Laxminarayan R, Matsoso P, Pant S, et al. Access to effective antimicrobials: a worldwide challenge. *Lancet*. 2016;387:168–175. https://doi.org/10.1016/S0140-6736(15)00474-2.
2 Theuretzbacher U, Outterson K, Engel A, Karlén A. The global preclinical antibacterial pipeline. *Nat Rev Microbiol*. 2020;18:275–285. https://doi.org/10.1038/s41579-019-0288-0.
3 World Health Organization. Global Action Plan on Antimicrobial Resistance, 978 92 4 150976 3; Geneva: World Health Organization; 2015.
4 Prioritization of pathogens to guide discovery, research and development of new antibiotics for drug-resistant bacterial infections, including tuberculosis; Geneva: World Health Organization; 2017.
5 Barriere SL. Clinical, economic and societal impact of antibiotic resistance. *Expert Opin Pharmacother*. 2015;16:151–153. https://doi.org/10.1517/14656566.2015.983077.
6 Tumbarello M, Viale P, Viscoli C, et al. Predictors of mortality in bloodstream infections caused by Klebsiella pneumoniae carbapenemase-producing K. pneumoniae: importance of combination therapy. *Clin Infect Dis*. 2012;55:943–950. https://doi.org/10.1093/cid/cis588.
7 Laxminarayan R, Duse A, Wattal C, et al. Antibiotic resistance—the need for global solutions. *Lancet Infect Dis*. 2013;13:1057–1098. https://doi.org/10.1016/S1473-3099(13)70318-9.
8 Nordmann P, Dortet L, Poirel L. Carbapenem resistance in Enterobacteriaceae: here is the storm!. *Trends Mol Med*. 2012;18:263–272. https://doi.org/10.1016/j.molmed.2012.03.003.
9 Shields RK, Potoski BA, Haidar G, et al. Clinical outcomes, drug toxicity, and emergence of ceftazidime-avibactam resistance among patients treated for carbapenem-resistant enterobacteriaceae infections. *Clin Infect Dis*. 2016;63:1615–1618. https://doi.org/10.1093/cid/ciw636.
10 2019 Antibacterial Agents in Clinical Development: An Analysis of the Antibacterial Clinical Development Pipeline; Geneva: World Health Organization; 2019.
11 Kalinin DV, Holl R. Insights into the zinc-dependent deacetylase LpxC: biochemical properties and inhibitor design. *Curr Top Med Chem*. 2016;16:2379–2430. https://doi.org/10.2174/1568026616666160413135835.
12 Supuran CT, Carta F, Scozzafava A. Metalloenzyme inhibitors for the treatment of Gram-negative bacterial infections: a patent review (2009–2012). *Expert Opin Ther Pat*. 2013;23:777–788. https://doi.org/10.1517/13543776.2013.777042.
13 Kalinin DV, Holl R. LpxC inhibitors: a patent review (2010–2016). *Expert Opin Ther Pat*. 2017;27:1227–1250. https://doi.org/10.1080/13543776.2017.1360282.
14 Shen S, Kozikowski AP. Why hydroxamates may not be the best histone deacetylase inhibitors—what some may have forgotten or would rather forget? *ChemMedChem*. 2016;11:15–21. https://doi.org/10.1002/cmdc.201500486.
15 Smith GF. Designing drugs to avoid toxicity. *Prog Med Chem*. 2011;50:1–47. https://doi.org/10.1016/B978-0-12-381290-2.00001-X.
16 Serio AW, Kubo A, Lopez S, et al. Structure, Potency AND Bactericidal Activity of ACHN-975, a First-In-Class LpxC Inhibitor. In 53rd Interscience Conference on Antimicrobial Agents and Chemotherapy; Achaogen; 2013 [poster #F-1226].
17 Shoji M, Suzumura Y, Fujiwara M, Kurosaki C, Nozaki Y, Mizunaga S. T-1228 (RC-01), A New LpxC Inhibitor Exhibiting Potent Activity against Multidrug-Resistant Gram-Negative Pathogens: Design, Synthesis and Structure-Activity Relationship. Presented at ASM Microbe, June 20−24, San Francisco, CA, USA, Sunday-AAR-740; 2019.
18 US National Library of Medicine. ClinicalTrials.gov, https://clinicaltrials.gov/ct2/show/NCT01870245; 2013.
19 US National Library of Medicine. ClinicalTrials.gov, https://clinicaltrials.gov/ct2/show/NCT03832517; 2019.
20 Yamada Y, Takashima H, Walmsley DL, et al. Fragment-based discovery of novel non-hydroxamate LpxC inhibitors with antibacterial activity. *J Med Chem*. 2020;63:14805–14820. https://doi.org/10.1021/acs.jmedchem.0c01215.
21 Lee CJ, Liang X, Chen X, et al. Species-specific and inhibitor-dependent conformations of LpxC: implications for antibiotic design. *Chem Biol*. 2011;18:38–47. https://doi.org/10.1016/j.chembiol.2010.11.011.
22 Brown DG, May-Dracka TL, Gagnon MM, Tommasi R. Trends and exceptions of physical properties on antibacterial activity for gram-positive and gram-negative pathogens. *J Med Chem*. 2014;57:10144–10161. https://doi.org/10.1021/jm501552x.
23 Piizzi G, Parker DT, Peng Y, et al. Design, synthesis, and properties of a potent inhibitor of pseudomonas aeruginosa deacetylase LpxC. *J Med Chem*. 2017;60:5002–5014. https://doi.org/10.1021/acs.jmedchem.7b00377.
24 Surivet J-P, Panchaud P, Specklin J-L, et al. Discovery of novel inhibitors of LpxC displaying potent in vitro activity against gram-negative bacteria. *J Med Chem*. 2020;63:66–87. https://doi.org/10.1021/acs.jmedchem.9b01604.
25 Molecular Operating Environment (MOE), 2019.01; Chemical Computing Group ULC, 1010 Sherbooke St. West, Suite #910, Montreal, QC, Canada, H3A 2R7; 2018.
26 Zhang J, Chan A, Lippa B, et al. Structure-based discovery of LpxC inhibitors. *Bioorg Med Chem Lett*. 2017;27:1670–1680. https://doi.org/10.1016/j.bmcl.2017.03.006.
27 Cohen F, Aggen JB, Andrews LD, et al. Optimization of LpxC inhibitors for antibacterial activity and cardiovascular safety. *ChemMedChem*. 2019;14:1560–1572. https://doi.org/10.1002/cmdc.201900287.
28 Clements JM, Coignard F, Johnson I, et al. Antibacterial activities and characterization of novel inhibitors of LpxC. *Antimicrob Agents Chemother*. 2002;46:1793–1799. https://doi.org/10.1128/AAC.46.6.1793-1799.2002.
29 Langsdorf EF, Malikzay A, Lamarr WA, et al. Screening for antibacterial inhibitors of the UDP-3-O-(R-3-hydroxymyristoyl)-N-acetylglucosamine deacetylase (LpxC) using a high-throughput mass spectrometry assay. *J Biomol Screening*. 2010;15:52–61. https://doi.org/10.1177/1087057109355319.
30 CLSI. Performance Standards for Antimicrobial Susceptibility Testing. 29th ed. CLSI supplement M100. Wayne, PA: Clinical and Laboratory Standards Institute; 2019.